

SAM-TR-68-106

AD 680842

**THE CALCULATION OF RETINAL BURN AND
FLASHBLINDNESS SAFE SEPARATION
DISTANCES**

R. G. ALLEN, Ph.D., et al.



Approved for Release by the
CLEARINGHOUSE
for the Central Intelligence Agency
Distribution Statement: Approved for Release

DDC
RECORDED
JAN 23 1969
REGULATED
C

**USAF School of Aerospace Medicine
Aerospace Medical Division (AFSC)
Brooks Air Force Base, Texas**

September 1968

**This document has been approved for public release and sale;
its distribution is unlimited.**

54

Qualified requesters may obtain copies of this report from DDC. Orders will be expedited if placed through the librarian or other person designated to request documents from DDC.

When U. S. Government drawings, specifications, or other data are used for any purpose other than a definitely related Government procurement operation, the Government thereby incurs no responsibility nor any obligation whatsoever; and the fact that the Government may have formulated, furnished, or in any way supplied the said drawings, specifications, or other data is not to be regarded by implication or otherwise, as in any manner licensing the holder or any other person or corporation, or conveying any rights or permission to manufacture, use, or sell any patented invention that may in any way be related thereto.

SEARCHED BY		WRITE SECTION	<input type="checkbox"/>
INDEXED		DIFF SECTION	<input type="checkbox"/>
SERIALIZED			<input type="checkbox"/>
JUSTIFICATION			
BY			
DISTRIBUTION/AVAILABILITY GROUPS			
GEN.	AVAIL.	SEC/W	SPECIAL

**THE CALCULATION OF RETINAL BURN AND FLASHBLINDNESS
SAFE SEPARATION DISTANCES**

R. G. ALLEN, Ph.D.*

T. J. WHITE, M.A.*

D. J. ISGITT, B.S.*

D. E. JUNGBAUER, B.S.*

J. H. TIPS, M.A.*

E. O. RICHEY, M.S.†

*Life Sciences Division, Technology Inc., San Antonio, Tex.

†Ophthalmology Branch, USAF School of Aerospace Medicine, Brooks Air Force Base, Tex.

This document has been approved for public release and sale;
its distribution is unlimited.

FOREWORD

This report was prepared in the Life Sciences Division, Technology Inc., San Antonio, Tex., and the Ophthalmology Branch, USAF School of Aerospace Medicine, in support of task No. 630103. The work was cosponsored by the Defense Atomic Support Agency under program element 6.16.46.01 D, project 5710, subtasks RMD 2003 and RMD 2134. It was accomplished between November 1966 and February 1968. The paper was submitted for publication on 25 June 1968.

This report has been reviewed and is approved.



GEORGE E. SCHAFER
Colonel, USAF, MC
Commander

ABSTRACT

This report describes a method for calculating safe separation distances from a nuclear fireball from the standpoint of permanent injury (chorioretinal burns) and temporary effects (flashblindness). Weapon characteristics, atmospheric transmission, and the interaction of radiant energy with the eye are discussed. Predicted safe separation distances from a nuclear flash for humans are presented as functions of observer altitude, height of burst, weapon yield, and day or night conditions.

CORRECTIONS

("The Calculation of Retinal Burn and Flashblindness Safe Separation Distances," by R. G. Allen et al., SAM-TR-68-106, Sept. 1968)

Page 23, TABLE IA: The title of the table should be "Values of $\underline{a}(\lambda, t^*)$."

Page 24, TABLE IA (contd.): The title of the table should be "Values of $\underline{a}(\lambda, t^*)$."

Page 24, TABLE IIA: The title of the table should be "Values of $\underline{b}(\lambda, t^*)$."

Page 25, TABLE IIA (contd.): The title of the table should be "Values of $\underline{b}(\lambda, t^*)$."

Page 25, TABLE IIA (contd.): In col. 5, items 13 and 14 (0.401 and 0.388) should have been at the bottom of the column and the remaining 7 entries should be moved up 2 spaces.

Page 26, par. 1, line 8: The word group should be changed to graph.

THE CALCULATION OF RETINAL BURN AND FLASHBLINDNESS SAFE SEPARATION DISTANCES

I. INTRODUCTION

It has been known for many years that damage to the eyes can occur as a result of viewing a very bright light, and that this damage could result in a permanent loss of visual acuity. The early evidence of retinal damage produced in this way was observed in individuals who had viewed a solar eclipse without adequate eye protection (1). The resulting loss in vision was called "eclipse blindness," and even now, despite frequent warnings to the public, injuries from viewing eclipses are still reported (2).

The development of nuclear weapons introduced a new and potentially more hazardous source of radiation capable of producing eye injuries. The potential for eye injury was recognized from the beginning, and protective goggles were worn at the first atomic bomb test in 1942—and in each test thereafter.

The first experiments dealing with the effects of a nuclear flash on the eyes were conducted by the USAF School of Aviation Medicine in 1951 during "Operation Buster." This problem was apparently not discussed in the open literature until 1953 when it was pointed out that, because of the focusing of energy by the eye, injury could be sustained at extremely long distances—much longer distances than those at which injury could be produced by any other direct effects (3).

After "Operation Buster" came a series of field experiments to study the effects of nuclear detonations on vision. This series of field studies culminated with an extensive experiment conducted during "Operation Dominic" and "Operation Fishbowl" in 1962 (4).

Today, there are several sources of radiant energy that are capable of producing retinal damage, and most of these sources possess a much greater capacity for producing damage than does the sun. With the possible exception of the Q-switched laser—an ultrahigh power mode of laser operation that may introduce a new spectrum of biologic damage (5, 6)—the mechanism by which injury to the eye is produced appears to be the same in all cases—viz, the production of regions of elevated temperatures in the retina and adjacent regions as a result of absorption of the incident radiant energy. Since permanent injury appears to be simply a consequence of generating excessive temperatures, no matter whether the source is the sun, a nuclear detonation, a normally operated laser, a pulsed xenon tube, an incandescent plasma, or some other high intensity source, the damage produced will be similar in each case—differing only as a result of variations in the conditions of exposure, differences in the characteristics of the sources, and differences in the subjects themselves.

The significance of chorioretinal burns depends upon a number of factors. Some of these factors are associated with the physical characteristics of the actual lesions—such as size, location, and severity. These factors determine the particular visual function affected and the extent of loss of function. In contrast, other factors involve the consequences of having suffered a loss of visual function. These factors deal with the importance to the individual of the specific function affected, the extent of the functional loss, the possibility of partial recovery, and the potential for partly overcoming the loss by visual training and practice.

II. GENERAL DISCUSSION

This report was developed for use in determining acceptable proximity to nuclear detonations from the standpoint of eye effects. The two potential visual hazards dealt with are retinal burns and flashblindness. Weapon yields from 0.01 KT to 10 MT at burst, and flight altitudes ranging from sea level to 50,000 ft. have been considered.

The distances determined using the retinal burn envelopes are the minimum allowable distances from fireball to observer that are considered "safe"—i.e., distances at which no permanent damage will be produced for the exposure times under consideration.

The distances determined using the flashblindness envelopes are also minimum allowable distances, but in this case, they refer to temporary rather than permanent visual impairment. These curves describe the distance at which 10 seconds of flashblindness will be experienced—i.e., distances at which it will take 10 seconds to recover sufficient acuity to obtain useful information from flight instruments.

Weapon characteristics, atmospheric transmission, and pertinent aspects of the physiology of vision are discussed cursorily in order to acquaint the reader with the basic concepts involved and to relate retinal exposure to loss of visual function.

Weapon characteristics

There are several basic differences between nuclear and conventional high-explosive weapons. A nuclear explosion may be many times more powerful than the largest conventional explosion; it is accompanied by highly penetrating ionizing radiations. The fission products remaining after a nuclear detonation are radioactive, and a very large amount of nuclear energy is converted to thermal energy (light and heat). It is the thermal energy that is responsible for chorioretinal burns and flashblindness.

Figure 1 shows the distribution of energy from a fission weapon in a typical air burst. For detonations in the atmosphere below 50,000 ft., the fraction of energy converted to thermal energy lies between 30% and 40% (7).

At lower altitudes, a gaseous fireball is formed and essentially all of the thermal energy is emitted in two pulses (fig. 2). The first is relatively short and contains less than 1% of the total energy. The second pulse, which contains almost all of the energy, is much longer. Although the first pulse contains less than 1% of the energy, under certain circumstances it is capable of producing permanent injury to the retina. For detonations at higher altitudes, more of the thermal energy appears in the first pulse. For very high altitude detonations, essentially all of the energy is emitted in a single, very short pulse.

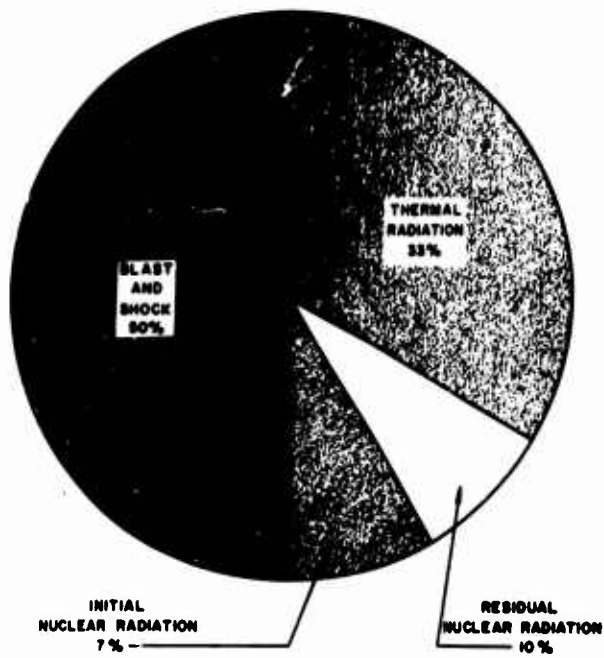


FIGURE 1

Distribution of energy in a typical air burst nuclear detonation.

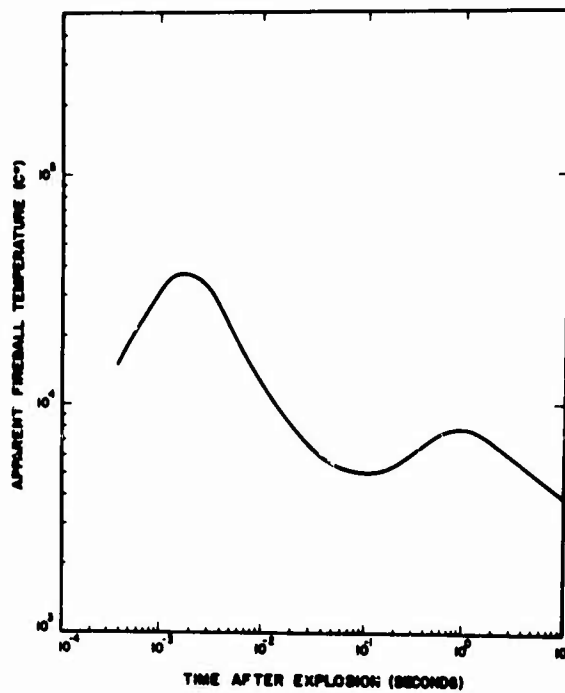


FIGURE 2

Apparent fireball temperature as a function of time after detonation.

The amount of thermal energy arriving at the position of the observer depends upon the weapon design and size, altitude of the detonation, distance to and altitude of the observer, and characteristics of the intervening atmosphere. Estimation of this energy comprises a large part of the problem of predicting safe separation distances.

Atmospheric transmission

Before reaching the eye, the radiant energy emitted by the fireball is attenuated by the atmosphere through processes of scattering and absorption. Attenuation by the atmosphere is a subject of some complexity because of the variety of phenomena and situations which can be involved. In general, attenuation of radiant energy by the atmosphere depends upon the composition, characteristics, and distribution of the atmosphere in the path between detonation and observer and the energy spectrum of the emitted radiation. These atmospheric factors vary from time to time and place to place and frequently are difficult or impossible to predict with any accuracy. For the problem of retinal burns, it does not appear necessary to consider all of the phenomena involved, or to account for the full range of situations and variations which can occur. Thus, consideration has been limited to the unscattered or image-forming radiation.

Interaction of radiant energy with the eye

The effects of thermal radiation on the eyes may be classified as permanent (chorioretinal burns) or temporary (flashblindness). Concentration of thermal energy on the retina by the eye lens system can result in injury to the retina; however, this will normally occur only if the source of energy is in the field of vision so that an image of the source is formed on the retina. Because of the focusing of energy by the eye, the distances at which chorioretinal burns can occur may be much greater than those at which thermal radiation produces skin burns. This comes about as follows: the irradiance (energy per unit area per unit time) incident on the eye is inversely proportional to the square of the distance from the fireball; however, the area of the fireball image on the retina is also inversely proportional to the square of the distance from the fireball. As a result, the irradiance at the retina in the image of the fireball is independent of the distance from the fireball—except for the effect introduced by atmospheric attenuation. Fortunately, atmospheric attenuation increases with distance so that distance can provide protection. Two other factors, pupil size and blink time, enter into the problem in a significant way. To admit more light, the pupil of the eye normally enlarges at low levels of illumination. Thus, under conditions of low ambient illumination (dusk or night) the pupil will be larger than in daylight and will allow more of the thermal energy from the fireball to reach the retina. Average pupil diameters assumed here are 5.8 mm. (night) and 2.5 mm. (day).

When considering blink time, it is apparent that only radiation received prior to closing the eyes in a reflexive blink can contribute to the production of retinal damage. As a result, the time for a blink to occur can be important.

III. RESULTS OF EXCESSIVE EXPOSURES

Chorioretinal burns

A sketch of the human eye is shown in figure 3. For purposes of discussion, the eye may be compared to a camera. Light rays received by the eye are refracted by the

cornea, lens, and ocular media so that they are focused on the retina where an image of the fireball is produced.

Mechanism of production. Heat generated in the retina and adjacent structures will in time diffuse away from the area in which the image is focused and will also be conducted away by the flow of blood in the vascular bed. If the rate of heat diffusion in an area is less than the rate of heat generation in that area, the temperature will increase. If the temperature exceeds the biologic tolerances for the area involved, injury to the photoreceptors (rods and cones), optical nerve tissue, and other structures in the retina and choroid may result—with a subsequent permanent loss of vision. Current research efforts are attempting to define threshold temperatures, but relatively little reliable quantitative information exists at present. Until more knowledge is gained in this area, it will be necessary to base threshold criteria upon visual retinal changes, histopathologic findings, or loss of function.

Effects on vision. The degree of visual impairment caused by a retinal burn will be dependent on the size, severity, and location of the burn. The size of the image, which

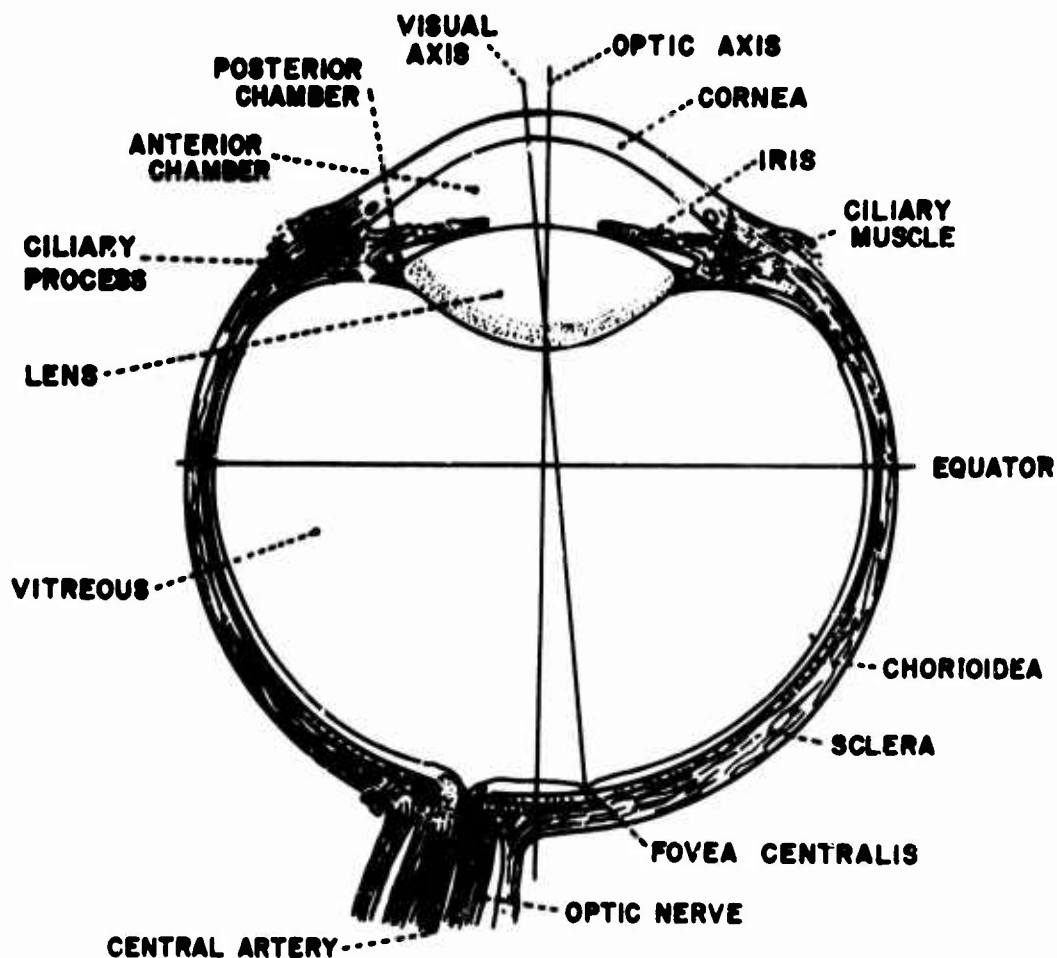


FIGURE 8

Schematic drawing of eye.

influences the size of a burn, depends on the visual angle subtended by the object—i.e., the size of the fireball and its distance from the observer. The severity of a burn depends, in general, upon the amount by which the exposure exceeds the threshold exposure. The function affected will be determined by the location of the burn. For example, a large burn in the fovea would seriously affect visual acuity, since the fovea is employed for high acuity and color recognition. A burn in the periphery would have less effect on visual acuity and, barring complications, could result in a scotoma or blind spot that would not normally be noticed. From figure 4, it can be estimated that burns exactly centered in each fovea and large enough to include the central 2.5-degree visual field would reduce visual acuity to about 57% of normal (20/35 on the Snellen scale). In theory, if the central 10-degree visual field were destroyed, the acuity would be 29% (20/70). Even if the central 20 degrees of vision were destroyed (an extremely unlikely situation), visual acuity would be reduced only to approximately 20% (about 20/100).

A schematic drawing of central field defects and the burns responsible for these defects is shown in figure 5. The burns numbered 1 to 6 are shown in the region of the macula as they would appear in size and relation to the optic nerve. Burns having

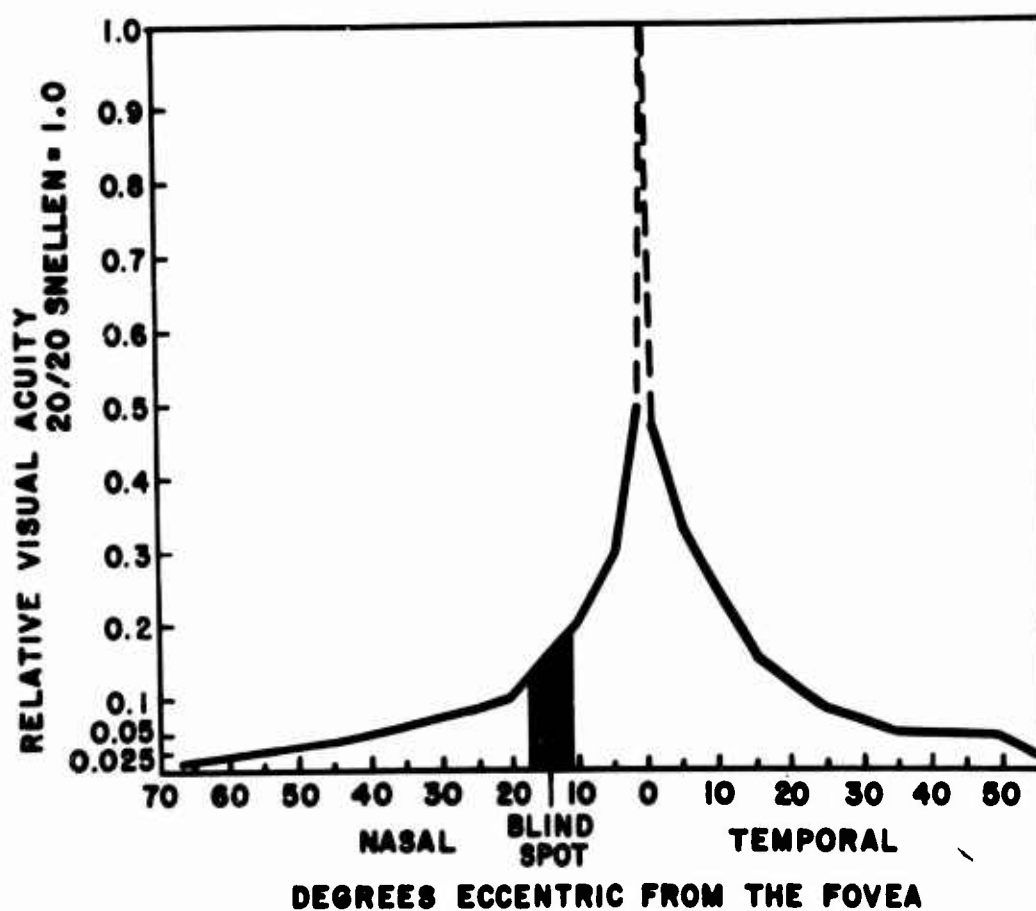


FIGURE 4

Visual acuity as a function of angular distance from the fovea.

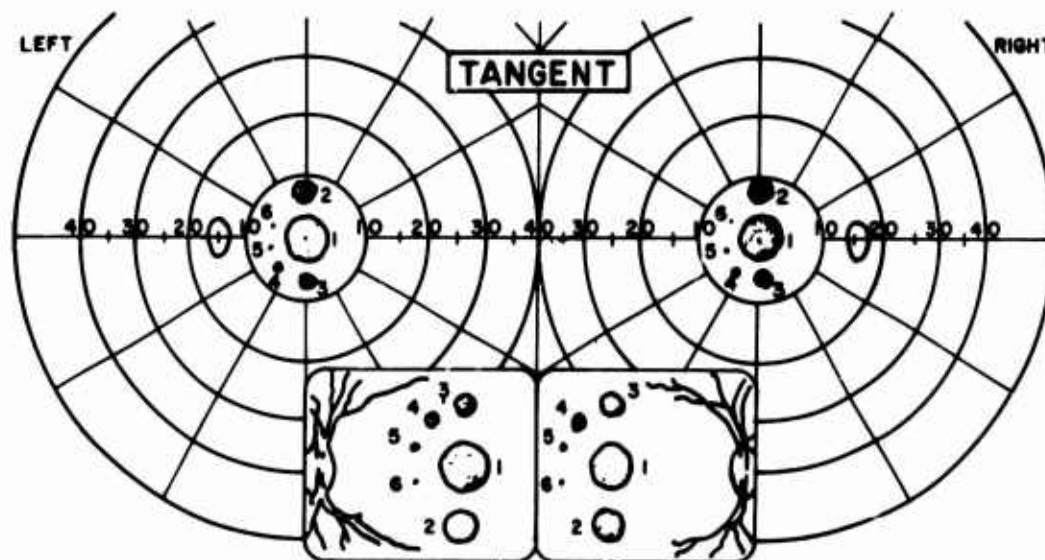
corresponding numbers result from a bilateral view of a single source. Corresponding scotomata are plotted on the field charts. The centrally located 1.8-mm. (6-degree) burn would cause a permanent visual impairment of approximately one-half to three-fourths of normal if centered on the fovea. Visual acuity would probably be no better than 20/60 even after edema has subsided. Burns located off the fovea should not reduce acuity, but only produce blind spots.

Extrafoveal burns may produce visual defects that are significantly different from foveal burns. Since a lesion of the nerve fiber layer produces a defect which corresponds to the area which is served by the affected fibers and not the area of the lesion, a small heavy burn near the disc could cause an extensive field defect as well as a localized scotoma at the site of the burn. The course of the nerve fibers of the retina is shown schematically in figure 6. Figure 7 shows field defects produced by damage to nerve fiber bundles.

The loss of vision resulting from retinal burns, although permanent and uncorrectable, does not take the form of total blindness. Burns can result in some impairment of vision in the form of blind "spots," but complete visual incapacitation as a result of retinal burns is extremely unlikely.

Flashblindness

The temporary decrease in visual sensitivity after exposure to a bright light has been termed "flashblindness," and the time required to regain visual function is called "recovery time." In considering recovery time, it is necessary to specify the visual task or



1. - 1.8 mm BURN CAUSING CENTRAL SCOTOMA OF 6°
2. - 1.35 mm BURN CAUSING PARACENTRAL SCOTOMA OF 4.5°
3. - .9 mm BURN CAUSING PARACENTRAL SCOTOMA OF 3°
4. - .45 mm BURN CAUSING PARACENTRAL SCOTOMA OF 1.5°
5. - .15 mm BURN CAUSING PARACENTRAL SCOTOMA OF 0.5°
6. - .07 mm BURN CAUSING PARACENTRAL SCOTOMA OF 0.25°

FIGURE 5

Schematic drawings of bilateral burns and resulting visual field defects.



FIGURE 6

Schematic drawing of the nerve fibers of the retina.

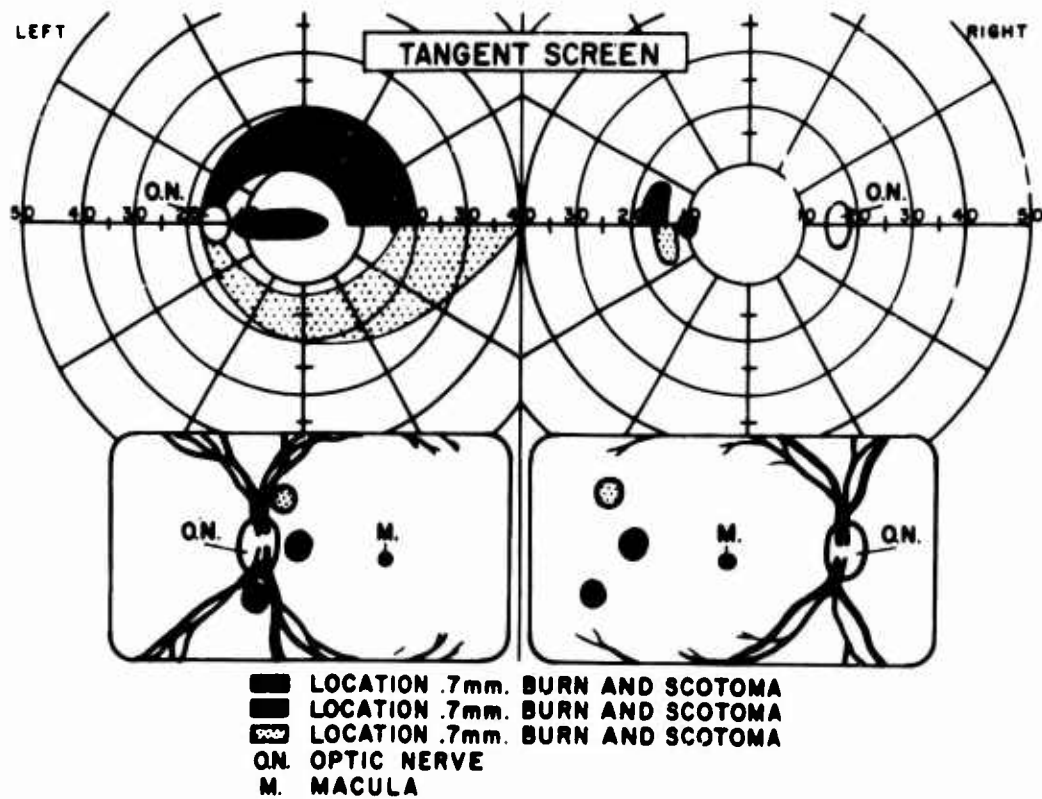


FIGURE 7

Schematic drawing of visual field defects resulting from injury to nerve fiber bundles.

the particular visual capability desired since the time required to reach a given level of visual performance depends upon the performance level selected.

Mechanism of production. Briefly, high-luminance lights produce afterimages of the shape and size of the primary images. The initially perceived brightness of an afterimage appears to be related to the amount of photopigment bleached in the area covered by the image, and the decrease in afterimage brightness with time appears to be related to the regeneration of the photopigments. An afterimage appears as a bright area in the visual field (or a dark area, depending upon the luminance of the background) and reduces contrast in a scene subsequently imaged within the area occupied by the afterimage. In order for an object to be seen "through" the afterimage, the object must produce a primary image of sufficient brightness to create a detectable contrast. Against the background of an afterimage, detail that could be detected prior to a flash may be indistinguishable until the afterimage decays to a brightness level permitting perceivable contrasts. As a result, recovery time depends generally upon the integrated incident luminous energy, the luminance of the subsequent scene, and the visual acuity required for perception of the particular detail desired.

Effects on vision. Figure 8 shows the general form of recovery time as a function of stimulus flash energy—assuming a constant flash duration (8). Target luminance is the parameter between curves. For very low flash energies, there will be no significant effect on visual function. As flash energy is increased, however, an increase in

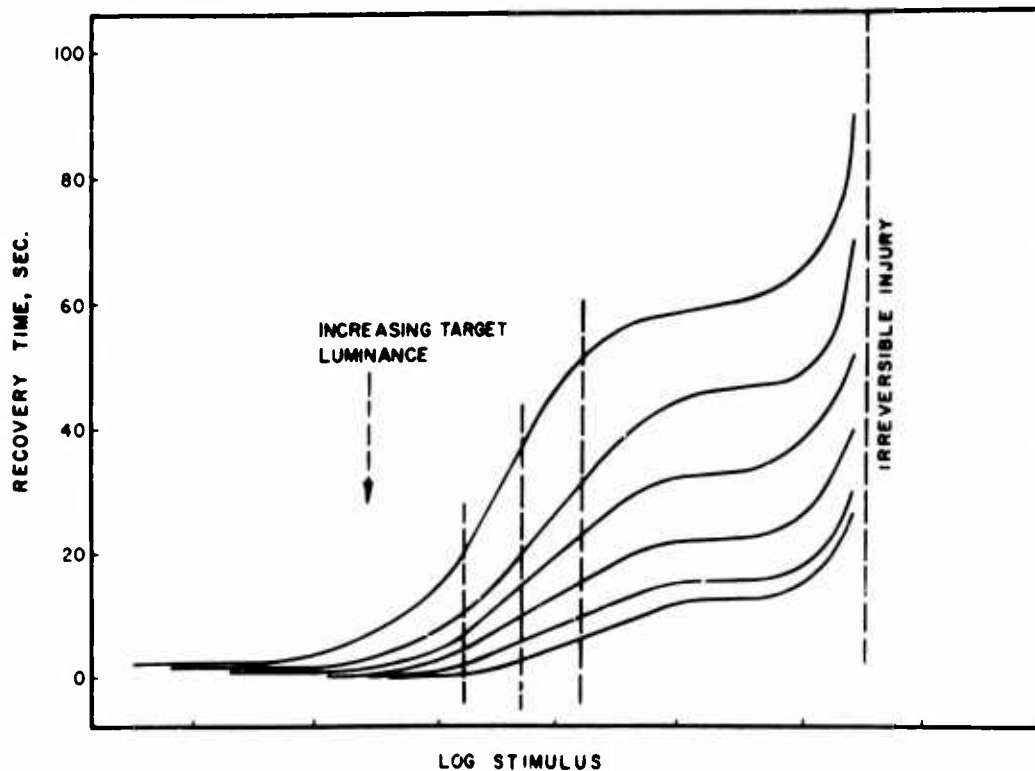


FIGURE 8

Effect of flash energy and display luminance on flashblindness recovery time.

recovery time becomes apparent. Recovery times may change very little with an increase in flash energy for exposure levels beyond those at which maximum bleaching occurs. As the flash energy approaches the threshold for injury, recovery time increases rapidly until injury occurs. At this point, function is lost irreversibly.

The relationship between target luminance and recovery time can also be inferred from an examination of figure 8. Increasing display luminances are represented by successively displaced curves in the figure. Recovery times decrease with increasing target luminance. Clearly, target luminance is an important variable and recovery times can be significantly reduced by increasing target luminance.

IV. MATHEMATICAL MODEL AND PREDICTION TECHNIQS

Retinal burns

Whether or not an observer will receive a retinal burn depends upon whether or not the retinal radiant exposure (Q_r) exceeds the threshold exposure (Q_c). Thus, the problem of calculating a safe separation distance is simply that of determining the distance at which $Q_r = Q_c$.

Determination of Q_r . The first problem is to establish the "source term"—i.e., the power output of the weapon as a function of time and wavelength for any yield. Spectral power may be written

$$P_\lambda = a(\lambda, t^*) W^{b(\lambda, t^*)} \quad (1)$$

where

W = Yield (kilotons).

P_λ = Spectral power $\left(\frac{\text{cal}}{\text{sec}-\mu} \right)$.

$t^* = \frac{t(\text{sec})}{t_{2\text{max}}} = \frac{t(\text{sec})}{0.037W^{0.47}} \cdot \left(\frac{\rho_0}{\rho_H} \right)^{0.282}$ and is called the scaled time.

t = Real time (sec.)

$t_{2\text{max}} = 0.037W^{0.47} \cdot \left(\frac{\rho_H}{\rho_0} \right)^{0.282}$

ρ_0 = Density of atmosphere at sea level.

ρ_H = Density of atmosphere at burst height.

The coefficients $a(\lambda, t^*)$ and the exponents $b(\lambda, t^*)$ reflect actual weapon experience and have been compiled for ten discrete wavelength bands (appendix A). The altitude dependence of the power term has been taken into account by the inclusion of the atmospheric density factor in the expression for scaled time (9). As the burst height of a given weapon increases, the scaled time also increases; this corresponds to the fact that the real time required to release a specified amount of energy decreases with increasing altitude.

Because the computer program uses spectral radiance, N_λ , instead of spectral power, it is necessary to calculate the fireball diameter, FD , as a function of time, yield, and

burst height. Experimental fireball data, as well as theoretical computations, were used in deriving the following scaling relationship:

$$FD(t^*, W) \text{ (cm)} = 0.3504 FD_s(t^*) W^{0.85} \cdot \left(\frac{\rho_o}{\rho_H}\right)^{0.18} \quad (2)$$

where

$FD(t^*, W)$ = Actual fireball diameter (in cm.) at scaled time t^* and yield W .

$FD_s(t^*)$ = Scaled fireball diameter (in cm.) determined from experiments (fig. 9).

This expression should be reasonably valid over the range of yields and burst altitudes considered in this report.

With spectral power, P_{λ_1} , and fireball diameter, $FD(t^*)$, determined, the spectral radiance, N_{λ_1} , is computed as follows:

$$N_{\lambda_1}(W, \lambda_1, t_j^*) \left(\frac{\text{cal}}{\text{cm}^2\text{-sec-}\mu\text{-}\Omega}\right) = \frac{P_{\lambda_1}(W, \lambda_1, t_j^*)}{[\pi FD(t_j^*, W)]^2} \quad (3)$$

Retinal irradiance is calculated for all times of interest, t_j^* , at a given horizontal range, S :

$$H_r(t_j^*, S) \left(\frac{\text{cal}}{\text{cm}^2\text{-sec}}\right) = \frac{\pi}{4} \cdot \left(\frac{PD}{FL}\right)^2 \sum_{i=1}^{10} N_{\lambda_1}(W, \lambda_i, t_j^*) T(\lambda_i, D) \Delta\lambda_i \quad (4)$$

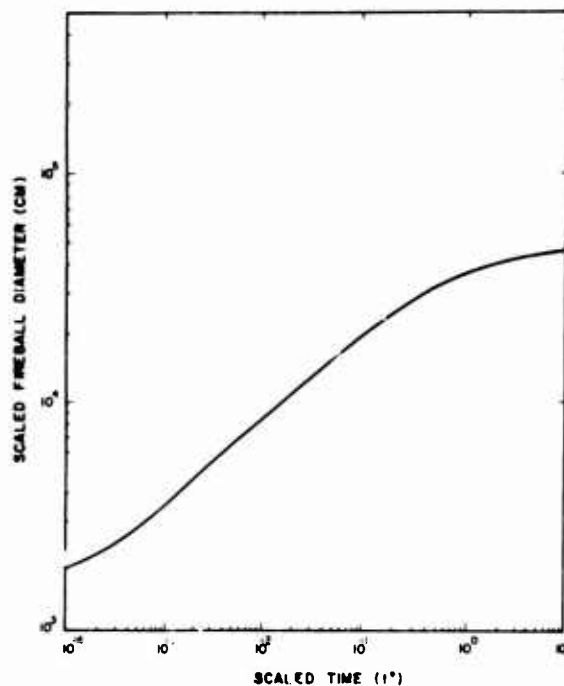


FIGURE 9

Scaled fireball diameter as a function of scaled time.

where

PD = Pupil diameter of the human eye (night: 5.8 mm.; day: 2.5 mm.).

FL = Effective focal length of the human eye (17 mm.).

$T(\lambda_i, D)$ = Transmission through a distance D of the atmosphere plus that of any canopies or filters, and the ocular media for the spectral band centered at λ_i .

D = Slant range (cm.).

$\Delta\lambda_i$ = Bandwidth of the i th spectral band (μ).

From the retinal irradiance at t_{j-1}^* , and that at t_j^* , the retinal radiant exposure for the time increment $\Delta t_j = (t_j^* - t_{j-1}^*) t_{2max}$ is determined, i.e.,

$$\Delta Q_{rj} \left(\frac{\text{cal}}{\text{cm}^2} \right) = \frac{H_r(t_j^*, S) + H_r(t_{j-1}^*, S)}{2} \cdot \Delta t_j \quad (5)$$

The total retinal exposure up to time t_j^* is then

$$Q_{rj} \left(\frac{\text{cal}}{\text{cm}^2} \right) = \sum_{j=1}^k \Delta Q_{rj}(t_j^*, S) \quad (6)$$

Equation 6 completes the determination of the retinal exposure as a function of distance and time. The problem of calculating $T(\lambda_i, D)$, however, remains. As noted earlier, the total transmission is composed of three parts: transmission through the atmosphere from fireball to observer, transmission through any canopies or filters, and transmission through the ocular media of the subject being considered.

Spectral transmission values for the ocular media of the human were obtained from Boettner and Wolter (10). It is assumed that no filters will be present to obstruct vision and that the spectral transmission values for an aircraft window taken from the "Operation Dominic" project report are representative for aircraft windshields (4).

Narrow beam transmission through the atmosphere is assumed, and this simplified model includes only scattering by air and water vapor. No account is taken of water vapor absorption and the effects of dust or other contaminants. Thus, transmission through this simplified atmosphere is given by

$$T_a(\lambda_i, D) = \left[T_{air}(\lambda_i) \right]^{AM} \left[T_{H_2O}(\lambda_i) \right]^W \quad (7)$$

where

$T_{air}(\lambda_i)$ = Transmission for pure dry air for 1 gm./cm.² in the spectral band centered at wavelength λ_i .

$T_{H_2O}(\lambda_i)$ = Transmission for one precipitable centimeter of water vapor (1 gm./cm.²) in the spectral band centered at wavelength λ_i .

AM = Number of grams per square centimeter of air in the direct path from fireball to observer.

W = Number of precipitable centimeters (grams per square centimeter) of water vapor in the direct path from fireball to observer.

$T_a(\lambda_i, D)$ = Total atmospheric transmission in the spectral band centered at wavelength λ_i for the direct path between the fireball and the observer.

$T_{\text{air}}(\lambda_1)$ and $T_{\text{H}_2\text{O}}(\lambda_1)$ are taken from the Smithsonian Meteorological Tables (11). In order to calculate AM and W, an integration along the slant path is made for the air and the water vapor density; that is,

$$\text{AM} \left(\frac{\text{gm}}{\text{cm}^2} \right) = \int_D \rho(h) dl \quad (8)$$

$$W \left(\frac{\text{gm}}{\text{cm}^2} \right) = \int_D \text{WVD} e^{-(\text{WLR})(h)dl} \quad (9)$$

where

$\rho(h)$ = Density of the atmosphere (gm./cm.^3) as a function of altitude, h (km.) (12).

dl = Element of slant path (in cm.) between detonation and observer.

WVD = Water vapor density at sea level (4) = $0.000022 \frac{\text{gm}}{\text{cm}^3}$.

WLR = Water vapor density lapse rate (4) = $0.5397 \frac{1}{\text{km}}$.

Figure 10 illustrates the quantities involved in the integration procedures. The program takes note of the sphericity of the earth and precludes the calculation of a separation distance that would lie beyond the horizon.

To calculate safe separation distances for a prescribed atmospheric visibility, the constants WVD and WLR in the equation for water vapor density as a function of altitude are modified. For a 10-km. visibility, WVD is given a value which will reduce the sea level transmission to 2% at 10 km. WLR is given a value so that the modified water vapor density is equal to the unmodified water vapor density when the two are compared at an altitude of 5 miles.

Determination of Q_c . The determination of the appropriate Q_c is accomplished using the burn threshold values measured by Technology Inc. (13). The measured burn thresholds (measured using rabbits) have been fitted with the expression:

$$Q_c \left(\frac{\text{cal}}{\text{cm}^2} \right) = \left[P_o(t) d_1^{-2} + H_o(t) \right] \cdot t \quad (10)$$

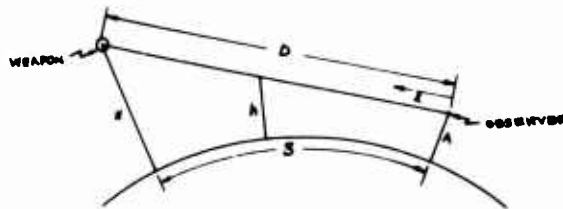


FIGURE 10

Geometry for calculation of atmospheric transmission.

where

d_i = Image diameter (mm.).

$P_o(t)$ and $H_o(t)$ = Tabular functions derived from experimental data.

Figure 11 shows the resulting curves for exposure times between 10^{-4} and 10 seconds. The difference between the way the laboratory threshold exposures were made and the way exposures from nuclear weapons occur necessitates careful consideration when comparisons are made.

At low altitudes, the fireball exhibits a typical two-pulse behavior; unfortunately the laboratory threshold exposure data were taken with single square pulse exposures. Thus, actual field data (with a continuously varying irradiance) and the laboratory data (with a constant irradiance) are not directly comparable. This is further complicated by the fact that the image increases in size with time in the case of a nuclear exposure, whereas the laboratory measurements were made with fixed size images.

The approach used here is to approximate the actual exposure during time t , with an exposure calculated as if it occurred under conditions similar to those in the laboratory—i.e., fixed size square pulse exposure. This is accomplished by determining an effective image diameter (d_i^{eff}) during the exposure time t and by assuming that the entire exposure occurs at the maximum retinal irradiance (H_r^{max}) experienced up to time t . In order to conserve the total retinal exposure (Q_r) an effective exposure time (t^{eff}) is established with the relationship:

$$t^{eff} = \frac{Q_r}{H_r^{max}} \quad (11)$$

The effective exposure time is calculated for each cumulative time and is used in equation 11 for the critical exposure Q_c . Because the total energy in the first pulse is less than 1% of the total energy in the second pulse, the calculation of t^{eff} is begun anew at the second pulse; i.e., Q_r is set equal to zero and any previous value of H_r is neglected.

The effective image diameter during the time t is established by weighting the actual image area as a function of time with the retinal irradiance (H_r). This places most emphasis on the image diameters that exist when the irradiance is greatest. The weighting is done conserving energy (ϵ_r) on the retina and assumes a uniform irradiance across the image:

$$\epsilon_r = A^{eff} \int_t H_r(t) dt = A^{eff} Q_r(t) = \int_t A(t) H_r(t) dt \quad (12)$$

where

$$A(t) = \frac{\pi}{4} [d_i(t)]^2 = \text{Area of the retinal image.}$$

$$A^{eff} = \frac{\pi}{4} [d_i^{eff}]^2 = \text{Area of the effective retinal image for time } t.$$

$$Q_r(t) = \text{Total retinal exposure at the center of the image for time } t.$$

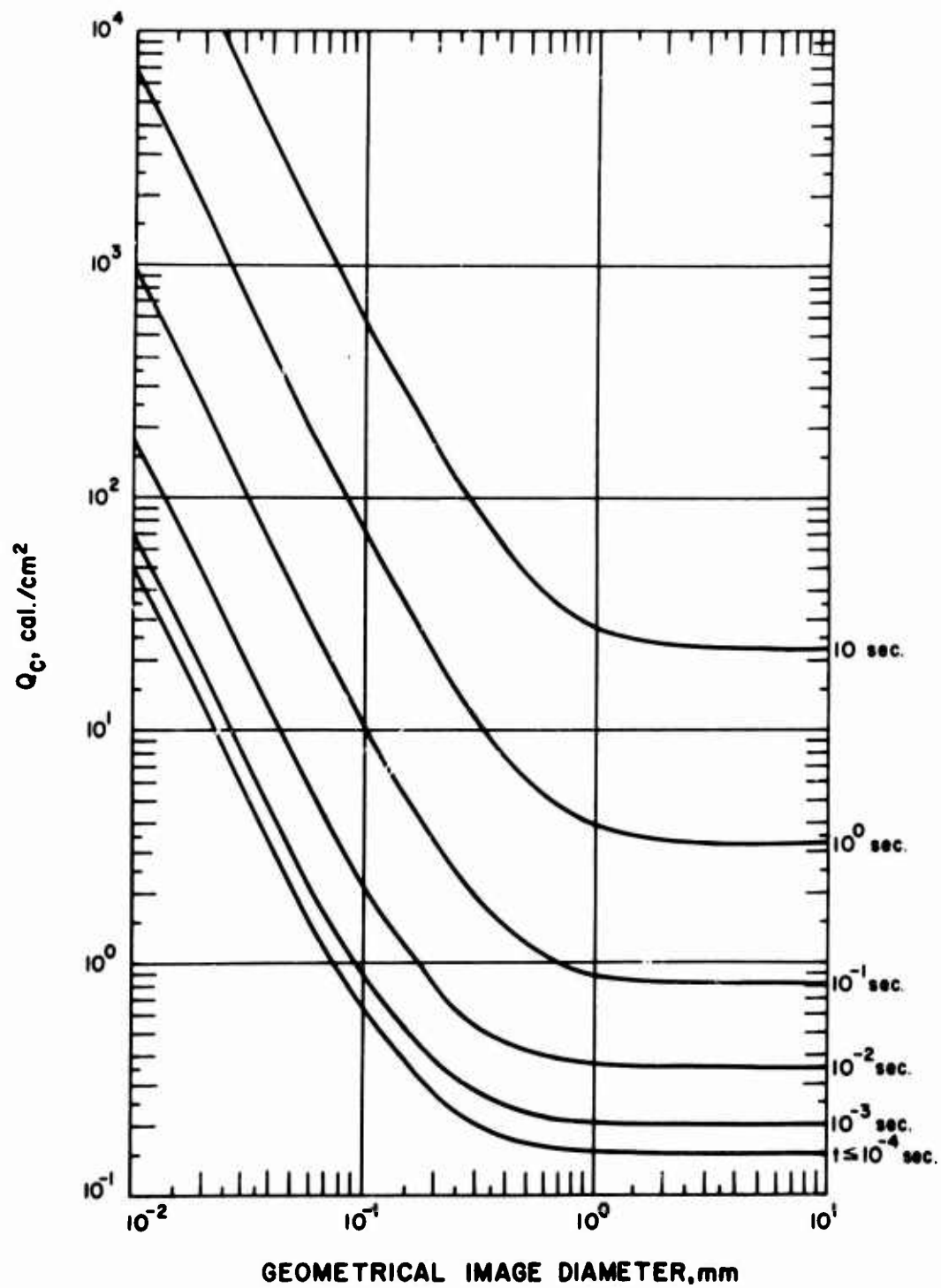


FIGURE 11

Threshold retinal exposure for rabbits as a function of geometrical image diameter and exposure time.

Upon rearrangement, the following expression is obtained for the effective image diameter:

$$d_i^{eff} = \left[\frac{\int [d_i(t)]^2 H_r(t) dt}{Q_r} \right]^{1/2} \quad (13)$$

Upon substituting the effective exposure time and the effective image diameter into equation 10, the following equation is obtained:

$$Q_c \left(\frac{\text{cal}}{\text{cm}^2} \right) = [P_o(t^{eff}) (d_i^{eff})^{-2} + H_o(t^{eff})] t^{eff} \quad (14)$$

Equations 6 and 14 complete the calculation of the retinal exposure and threshold exposure. A safety factor of 2 is applied to Q_r to account for inadequacies in the source data as well as approximations in the method. A safety factor of 4 is also applied to Q_c to take into consideration that the threshold data were obtained for burns appearing within 5 minutes after exposure on rabbits and minimal burns could appear at still later times and that the human fovea may be more sensitive than the rabbit fundus.

Convergence procedure. An iteration procedure has been established for finding the safe separation distance by determining the distance at which the quantities Q_c and Q_r are equal to each other.

Along with the yield, burst height, and other constants of the particular case, an approximation, S_o , to the maximum safe separation distance is read into the program as a simple device to decrease the number of iterations required to satisfy the convergence criteria. (This approximation is put into the program as an expedient only; any positive value would eventually produce a solution.) For the first time of interest, and for the first observer altitude, Q_r and Q_c are calculated as previously described for the input horizontal range, S_o . If $Q_r > Q_c$, S_o is incremented n times by $0.10 S_o$ until $Q_r < Q_c$. At this distance, $S_o + n(0.10 S_o)$, j successive increments and/or decrements (according to $Q_r < Q_c$ or $Q_r > Q_c$) of magnitude $\frac{0.10 S_o}{2^i}$ ($i = 1, 2, \dots, j$) are taken until the j th increment (decrement) is less than or equal to 1% of $S_o + n(0.10 S_o)$, with the additional restriction that $200 \text{ ft.} \leq \frac{0.10 S_o}{2^i} \leq 6,080 \text{ ft.}$ The distance for which the j th increment (decrement) satisfies the above criteria is the safe separation distance. If $Q_r < Q_c$, the initial distance S_o is successively incremented or decremented by $\frac{S_o}{2^i}$ ($i = 1, 2, \dots, k$) until the k th increment (decrement) is less than or equal to 1% of S_o , with the restriction that $200 \text{ ft.} \leq \frac{S_o}{2^i} \leq 6,080 \text{ ft.}$ That distance for which the k th increment (decrement) satisfies the stated criteria is the safe separation distance. An exactly analogous method is used for the remainder of the observer altitudes; but for the sake of efficiency, the final horizontal range that is found for a given observer altitude is taken as the initial range for the next observer altitude. With the completion of the above routine for all of the observer altitudes, the next time of interest is chosen; this entire process is repeated until all the times are considered and the calculation is finished.

Sample safe separation envelopes are presented in figure 12. Figure 13 shows the results of tests for retinal burns on rabbits during "Operation Dominic." Also shown are burn threshold distances predicted with the present model for the rabbit and safe separation distances extrapolated to man. Figure 14 shows the safe separation distance as a function of time for a selected case. Results for man for a number of specific situations are presented in appendix B.

Flashblindness

To ascertain whether an observer in a given situation will be "flashblinded" for more than a specified period of time, it is necessary to consider three factors: the image diameter, the direct-image exposure, and the extra-image exposure. Preliminary evidence by Richey (14) indicates that imperative visual information can be extracted from a typical aircraft instrument panel after exposure to a centrally fixated flash of light, provided the image subtends a visual angle less than 3 degrees. In view of this result, a focused image on the fovea of less than 0.9 mm. (0.9 mm. corresponds to a 3-degree visual angle) is considered to have no significant effect on the observer's ability to perform this kind of visual task. Therefore, the calculation of a safe separation distance for flashblindness is essentially reduced to one of finding the horizontal range at which the retinal exposure, E_r (trol_{eff}-sec), either direct or extra-image at 1.5 degrees from the fovea, is equal to the threshold retinal exposure, E_c (trol_{eff}-sec). The determination of E_r (with the assumption that the image is centered on the fovea—a worst case philosophy) and E_c is explained in the following sections.

Determination of E_r . Since the direct- and extra-image exposures are essentially products of different mechanisms, they will be dealt with separately in this section. The direct-image exposure will be calculated first.

Direct-image retinal exposure, E_r^d (trol_{eff}-sec), at a time t_k and at a horizontal range S is equal to the product of the time-integrated luminance of the source $\left(\frac{\text{cd-sec}}{\text{m}^2}\right)$ and the effective area of the observer's pupil (mm^2); i.e.,

$$E_r^d \text{ (trol}_{\text{eff}}\text{-sec)} = \frac{\pi}{4} (PD_{\text{eff}})^2 \sum_{j=1}^k \sum_{i=1}^{10} L_{\lambda_i}(\lambda_i, t_j^*) T_{\text{ax}}(\lambda_i, D) \Delta\lambda_i \Delta t_j \quad (15)$$

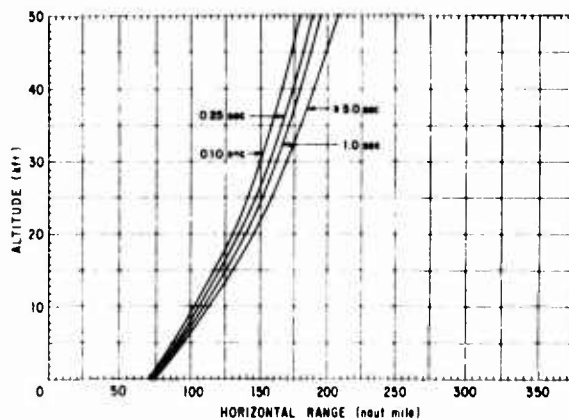


FIGURE 12

Example of retinal burn safe separation envelopes for a 10,000-KT detonation at 10,000 ft. during night hours with 100-km. visibility.

where

$$L_{\lambda_1}(\lambda_1, t_j^*) = \text{Spectral luminance of the fireball (in } \frac{\text{cd}}{\text{m}^2\text{-}\mu\text{)}} \text{ at time } t_j^* \text{ and for the bandwidth centered at } \lambda_1.$$

Equation 15 is used for the retinal exposure as long as the image diameter (at time t_x and at distance S) is larger than 0.9 mm. If the image diameter is less than 0.9 mm., the extra-image exposure is calculated.

The extra-image exposure is theoretically attributable to three separate sources: intraocular scattering, atmospheric scattering, and reflected energy from clouds, ground, and water. Because of the extreme range of conditions that can exist in actual situations, no account was taken of the exposure from clouds, ground, water, and other reflecting surfaces.

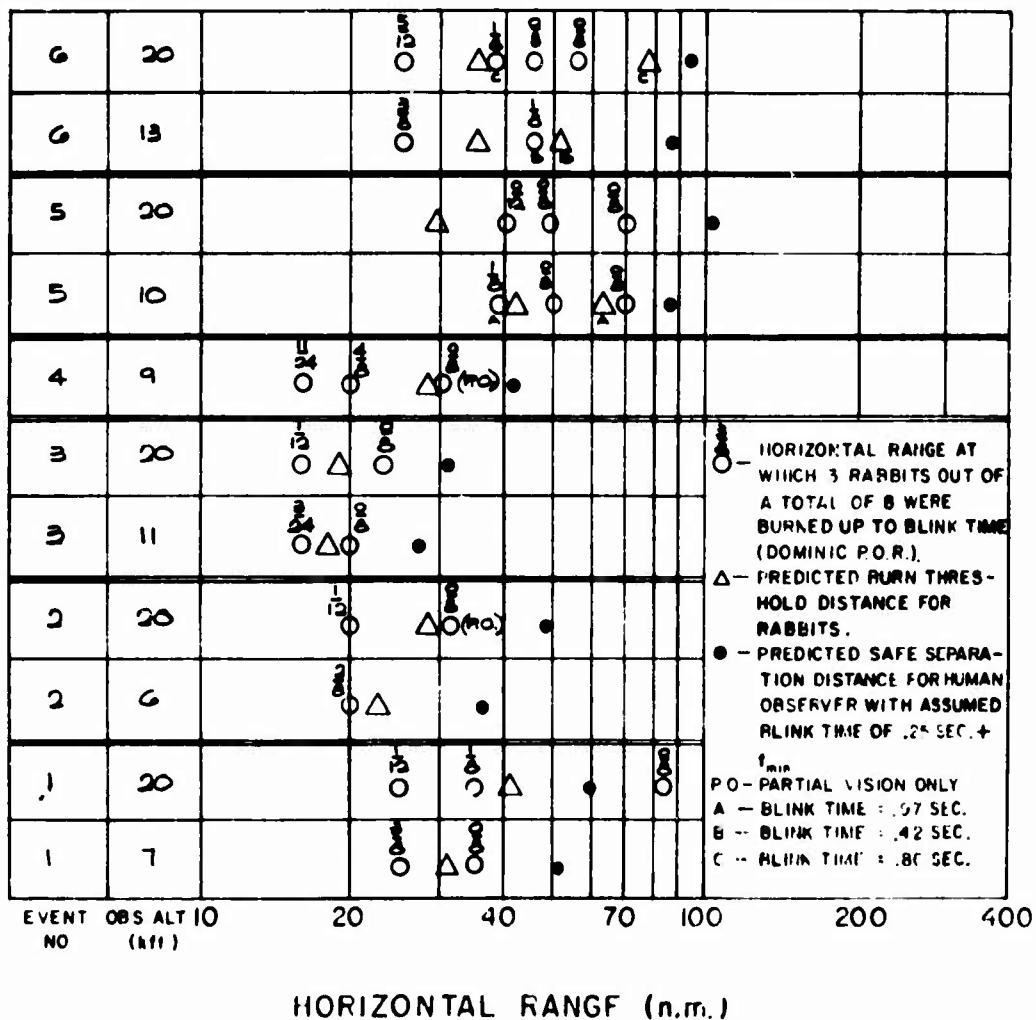


FIGURE 13

"Operation Dominic" burn threshold distances for rabbits and predicted safe separation distances for man.

Vos (15, 16) has derived an expression for intraocular scattering as well as one for atmospheric scattering, based on the following assumptions: (1) The fireball is a point source with respect to the scattered light. (2) The scattered light varies inversely with the square of the distance from fireball to the observer. (3) The extra-image exposure at a point on the retina is dependent upon the angle between that point and the direction of fixation (i.e., the direction of the fireball).

On the basis of the description by Vos, the extra-image retinal exposure, $E_o^{ex}(\text{trol}_{eff}\text{-sec})$, from the intraocular scattering may be calculated from the expression:

$$E_o^{ex}(\text{trol}_{eff}\text{-sec}) = \frac{9.87(PD_{eff})^2}{D^2\theta^2} \sum_{j=1}^k \sum_{l=-1}^{10} [FD_j(t_j^*, W)]^2 L_{\lambda_1}(\lambda_l, t_j^*) T_{ax}(\lambda_l, D) \Delta\lambda_l \Delta t_j, \quad (16)$$

while the exposure due to atmospheric scattering, $E_a^{ex}(\text{trol}_{eff}\text{-sec})$, is given by:

$$E_a^{ex}(\text{trol}_{eff}\text{-sec}) = \frac{-9.87(PD_{eff})^2}{D^2\theta} \times \sum_{j=1}^k \sum_{l=-1}^{10} [FD_j(t_j^*, W)]^2 L_{\lambda_1}(\lambda_l, t_j^*) T_{ax}(\lambda_l, D) \log_e T_a(\lambda_l, D) \Delta\lambda_l \Delta t_j, \quad (17)$$

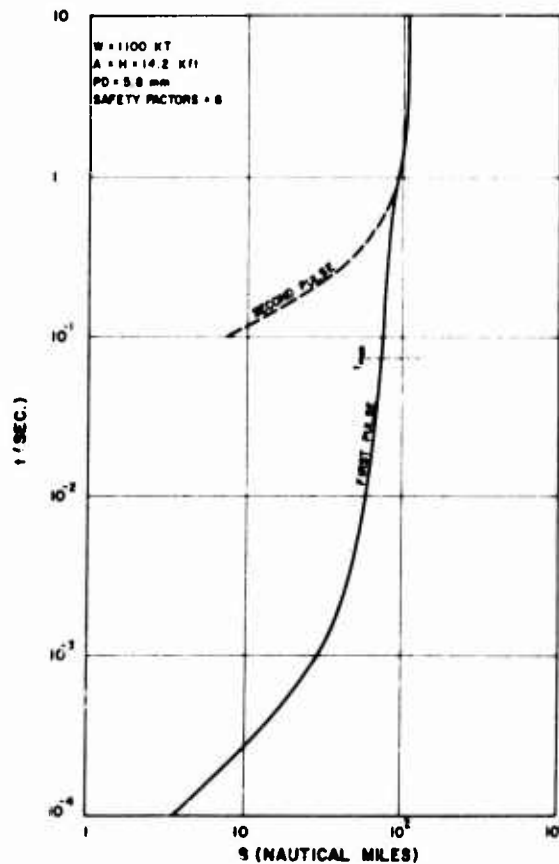


FIGURE 14

Retinal burn safe separation envelope as a function of time for a 1,100-KT detonation at night. Detonation and observer altitudes are both 14,200 ft.

where

E_o^{ex} = Extra-image exposure due to intraocular scattering at a time t_k and at a horizontal range S .

E_a^{ex} = Extra-image exposure due to atmospheric scattering at a time t_k and at a horizontal range S .

θ = Angle in degrees between the direction of fixation and the direction corresponding to the point at which the extra-image exposure is being calculated.

and all other quantities are as previously defined. Equations 15, 16, and 17 are the complete expressions for the direct- and extra-image exposures.

Critical exposure, E_c . The critical exposure used in calculating safe separation distances for flashblindness is that exposure for which the observer will be unable to perform a specified visual task for 10 seconds. It is evident from figure 8 that target or task luminance is a highly important variable in the determination of recovery time for a given stimulus. Therefore, a value of task luminance must be selected for both the day and the night conditions before a threshold exposure can be defined. The average instrument luminance under night conditions has been taken as 0.07 mL. (17), whereas that for day conditions is assumed to be 20 mL. (18). According to Miller (19), the foveal exposures corresponding to the above task luminances for 10-second recovery times are 7.87×10^6 trol_{ret}-sec and 1.97×10^7 trol_{ret}-sec, respectively. Reciprocity is assumed here, even though it is known that reciprocity does not hold over the entire range of interest. The transmission through the eye has not been included in the threshold exposures; so $T_{\lambda}(D)$ does not include the transmission of the clear media of the eye for any calculations of flashblindness.

As in the case of retinal burns, safety factors have been introduced into these calculations. A factor of 2 is again included in the calculated exposure values to compensate for possible errors in weapon output data. A factor of 2 is introduced into the threshold value to account for variations among individuals and the failure of reciprocity. Thus, the equation to be solved for "safe" separation for flashblindness is $4E_r = E_c$, where E_r is the luminous exposure at a position 1.5 degrees from the fovea, calculated by using equations 15 or 16 and 17, whichever is appropriate.

Convergence procedure. The retinal exposure (direct- and extra-image) and the critical exposure having been found, it remains to calculate the safe separation distance. Because of the requirement that the image diameter be greater than or equal to 0.9 mm., the first step in the convergence routine is to set the initial horizontal range to such a value, S_0 , that the image diameter is equal to 0.9 mm. The direct image retinal exposure is then calculated and compared with the appropriate threshold value (day or night). If E_r^d is within 1% of E_c , then the initial value S_0 is the safe separation distance. If $E_r^d < E_c$, then the value S_0 is initially decremented by $\frac{S_0}{2^i}$ and then either incremented or decremented until the i th increment or decrement is less than or equal to 1% of S_0 with the auxiliary condition that $200 \text{ ft.} \leq \frac{S_0}{2^i} \leq 6,080 \text{ ft.}$ That horizontal distance for which the i th increment or decrement satisfies the above criterion is then the safe separation distance. For $E_r^d > E_c$, the extra-image exposure, $E_o^{ex} + E_a^{ex}$, is calculated for $\theta = 1.5$ degrees and compared with E_c . If $E_o^{ex} + E_a^{ex} \leq E_c$, then S_0 is the flashblindness safe separation distance. If the extra-image exposure is greater than the

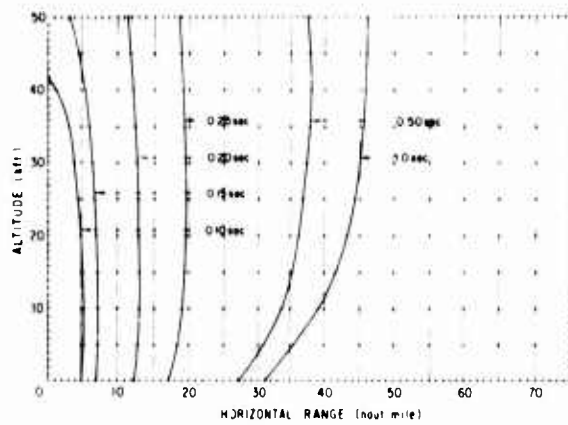


FIGURE 15

Example of flashblindness separation envelopes for a 100-KT detonation at 10,000 ft. during daylight hours with 100-km. visibility.

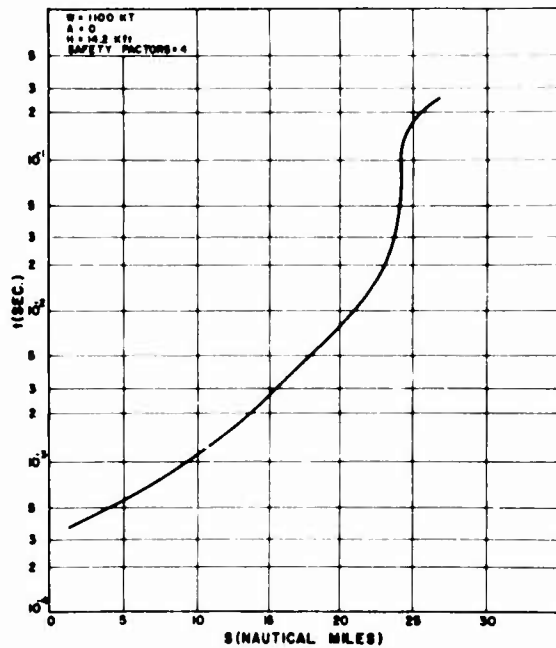


FIGURE 16

Flashblindness safe separation envelope as a function of time for a 1,100-KT detonation at 14,200 ft. with the observer at sea level.

threshold exposure, the initial distance, S_0 , is then successively incremented by S_0 until $E_0^{i+1} + E_e^{i+1} < E_c$; the horizontal range at that point, nS_0 , is then decremented by $\frac{S_0}{2^i}$ until the i th decrement is less than or equal to 1% of nS_0 (again with $200 \text{ ft.} \leq \frac{S_0}{2^i} \leq 6,080 \text{ ft.}$). The horizontal range that corresponds to the distance for the i th increment is the horizontal safe separation envelope as presented in figure 15. A curve of safe separation horizontal range versus time for flashblindness is given in figure 16. Results for a number of specific situations are presented in appendix C.

REFERENCES

1. Verhoeff, F. H., and L. Bell. The pathological effects of radiant energy on the eye. *Proc. Amer. Acad. Arts Sci.* 51:630 (1916).
2. Penner, R. Dept. of Ophthalmology, Walter Reed Army Hospital, Washington, D.C. Personal communication.
3. Buettner, K., and H. W. Rose. Eye hazards from an atomic bomb. *Sightsav. Rev.* 23:1 (1953).
4. Allen, R. G., Jr., et al. Production of chorioretinal burns by nuclear detonations and tests of protective devices and phototropic materials. (Unclassified title) POR 2014 (WT-2014). "Operation Dominic," project 4.1, Mar. 1965 (SECRET/FRD).
5. Felstead, E. B., and R. S. C. Cobbold. Analog solution of laser retinal coagulation. *Med. Electron Biol. Engin.* 3:145-155 (1965).
6. Zaret, M. M., et al. Laser coagulation of the eye. *Arch. Ophthal. (Chicago)* 69:97-104 (1963).
7. Glasstone, S. (ed.). *The effects of nuclear weapons*, revised ed. U.S. Government Printing Office, Washington, D.C., 1962.
8. Brown, J. L. Experimental investigation of flashblindness. *Hum. Factors* 6:503-516 (1964).
9. Darner, R. G. Systems and Electronics Division, Technology Inc., Dayton, Ohio. Personal communication, Sept. 1967.
10. Boettner, E. A., and J. R. Wolter. Transmission of the ocular media. *Invest. Ophthal.* 1:776 (1958).
11. List, R. J. *Smithsonian Meteorological Tables*. Smithsonian Institution, Washington, D. C., 1958.
12. U. S. standard atmosphere, 1962. U.S. Government Printing Office, Superintendent of Documents, Washington, D.C., 1962.
13. Allen, R. G., Jr., et al. Research on ocular effects produced by thermal radiation. Final report, USAF contract No. AF 41(609)-3099, July 1967.
14. Richey, E. O. Prediction of eye safe separation distances. Presented at AGARD Symposium on loss of vision from high intensity light, Paris, France, Mar. 1966.
15. Vos, J. J., et al. Some reflections on the danger of and the protection against nuclear flashblindness and retinal burns. Report No. IZF 1964-25, Institute for Perception RVO-TNO (AD 456-728), 1964.
16. Vos, J. J. Temporary and permanent loss of visual functions by flashes at nuclear explosions. A theoretical approach. Report No. 1959-7, Institute for Perception RVO-TNO (AD 332-591), 1959.
17. Handbook for instructions for aerospace personnel subsystem design (HIAPSD), AFSC Manual 80-3, 1 July 1961, report 15 Apr. 1965.
18. Pitts, D. G., and L. R. Loper. Ambient and cockpit luminance measurements. *Aerospace Med.* 34:145-149 (1963).
19. Miller, N. D. Visual recovery from high intensity flashes. Annual phase report, USAF contract No. AF 41(609)-2426, July 1965.

APPENDIX A

The equation for calculating the spectral power for a given wavelength and scaled time is

$$P(\lambda, t^*) = a(\lambda, t^*) W^{b(\lambda, t^*)}$$

where

$$P_\lambda = \text{Spectral power} \left(\frac{\text{cal}}{\text{sec} \cdot \mu} \right).$$

λ = Wavelength (μ).

t^* = Scaled time.

W = Yield (kilotons).

Tables IA and IIA contain the appropriate coefficients and exponents for selected wavelengths and scaled times. These values were determined from a reduction of the best available experimental nuclear weapon data.

Interpolation between scaled times should be done logarithmically on both axes; also, it is recommended that interpolation between wavelengths not be attempted until more spectral data are available.

TABLE IA
Values of $b(\lambda, t^*)$

t^*	λ (μ)					
	0.365	0.400	0.450	0.550	0.660	0.750
5.0E-4	5.90E 11	3.10E 11	2.62E 11	1.60E 11	9.30E 10	8.50E 10
7.5E-4	1.38E 12	8.30E 11	1.29E 12	5.90E 11	3.12E 11	2.20E 11
1.0E-3	2.10E 12	1.71E 12	2.80E 12	1.27E 12	6.00E 11	4.20E 11
2.0E-3	3.45E 12	5.20E 12	5.90E 12	4.35E 12	9.70E 11	6.60E 11
2.2E-3	3.62E 12	5.40E 12	6.10E 12	4.50E 12	9.80E 11	6.70E 11
5.0E-3	2.38E 12	4.10E 12	4.70E 12	3.39E 12	8.30E 11	5.58E 11
7.5E-3	1.61E 12	3.05E 12	3.45E 12	2.38E 12	6.41E 11	4.60E 11
1.0E-2	1.03E 12	2.17E 12	2.55E 12	1.79E 12	5.30E 11	3.65E 11
2.0E-2	3.32E 11	8.10E 11	1.11E 12	7.50E 11	3.05E 11	2.00E 11
5.0E-2	5.80E 10	1.80E 11	3.22E 11	2.79E 11	1.89E 11	1.54E 11
7.5E-2	2.20E 10	1.15E 11	1.85E 11	2.42E 11	1.90E 11	1.40E 11
1.0E-1	1.35E 10	9.20E 10	1.60E 11	2.40E 11	2.15E 11	1.80E 11
2.0E-1	1.35E 10	1.0E 11	2.00E 11	3.59E 11	3.60E 11	3.60E 11
5.0E-1	9.50E 11	2.30E 12	4.00E 12	3.42E 12	2.05E 12	1.50E 12
7.5E-1	2.20E 12	5.10E 12	6.60E 12	5.80E 12	2.92E 12	2.10E 12
1.0E 0	2.90E 12	6.10E 12	6.80E 12	6.50E 12	3.60E 12	2.30E 12
1.5E 0	2.30E 12	5.00E 12	6.20E 12	5.10E 12	3.60E 12	2.30E 12
2.0E 0	1.55E 12	3.43E 12	4.80E 12	3.80E 12	3.15E 12	2.10E 12
5.0E 0	2.30E 11	3.30E 11	1.1E 12	1.18E 12	1.10E 12	8.60E 11
1.0E 1	4.20E 10	4.70E 10	1.80E 11	3.86E 11	3.10E 11	2.70E 11
2.0E 1	5.60E 9	8.00E 9	5.20E 9	4.00E 10	6.30E 10	6.00E 10

TABLE IA (contd.)

Values of $b(\lambda, t^*)$

t^*	$\lambda (\mu)$				$\int a(\lambda, t^*) d\lambda$
	0.900	1.040	1.280	1.600	
5.0E-4	4.50E 10	2.95E 10	2.29E 10	9.10E 9	1.16E 11
7.5E-4	1.10E 11	4.85E 10	3.59E 10	1.37E 10	3.48E 11
1.0E-3	1.76E 11	6.90E 10	5.10E 10	1.69E 10	6.80E 11
2.0E-3	3.40E 11	1.20E 11	8.75E 10	2.75E 10	1.52E 12
2.2E-3	3.48E 11	1.25E 11	8.90E 10	2.90E 10	1.58E 12
5.0E-3	3.20E 11	1.42E 11	1.03E 11	4.40E 10	1.36E 12
7.5E-3	2.53E 11	1.37E 11	1.00E 11	4.95E 10	1.10E 12
1.0E-2	2.00E 11	1.26E 11	9.40E 10	5.15E 10	8.90E 11
2.0E-2	1.07E 11	9.50E 10	7.75E 10	5.50E 10	5.21E 11
5.0E-2	8.10E 10	7.50E 10	6.45E 10	5.90E 10	2.13E 11
7.5E-2	9.00E 10	7.60E 10	7.00E 10	6.20E 10	1.70E 11
1.0E-1	1.10E 11	8.60E 10	8.00E 10	7.00E 10	1.83E 11
2.0E-1	3.00E 11	1.43E 11	1.40E 11	1.30E 11	3.35E 11
5.0E-1	1.00E 12	3.95E 11	3.60E 11	4.00E 11	1.76E 12
7.5E-1	1.25E 12	5.60E 11	5.10E 11	5.30E 11	2.72E 12
1.0E 0	1.30E 12	6.60E 11	5.90E 11	5.70E 11	3.05E 12
1.5E 0	1.25E 12	7.00E 11	6.00E 11	5.60E 11	2.75E 12
2.0E 0	1.10E 12	6.55E 11	5.60E 11	4.70E 11	2.10E 12
5.0E 0	4.90E 11	3.60E 11	3.50E 11	1.20E 11	7.40E 11
1.0E 1	2.20E 11	1.35E 11	1.60E 11	3.80E 10	2.95E 11
2.0E 1	6.40E 10	4.20E 10	6.50E 10	1.90E 10	1.51E 11

TABLE IIA

Values of $a(\lambda, t^*)$

t^*	$\lambda (\mu)$					
	0.365	0.400	0.450	0.550	0.660	0.750
5.0E-4	0.510	0.653	0.725	0.860	0.878	0.853
7.5E-4	0.440	0.554	0.523	0.690	0.750	0.790
1.0E-3	0.381	0.451	0.418	0.590	0.661	0.650
2.0E-3	0.318	0.276	0.318	0.423	0.545	0.605
2.2E-3	0.375	0.288	0.310	0.423	0.595	0.608
5.0E-3	0.359	0.293	0.310	0.405	0.615	0.570
7.5E-3	0.368	0.305	0.331	0.423	0.605	0.540
1.0E-2	0.419	0.339	0.352	0.444	0.600	0.553
2.0E-2	0.482	0.323	0.360	0.460	0.551	0.595
5.0E-2	0.381	0.239	0.188	0.264	0.480	0.424
7.5E-2	0.482	0.251	0.218	0.172	0.397	0.396
1.0E-1	0.565	0.364	0.214	0.147	0.352	0.372
2.0E-1	0.635	0.398	0.410	0.117	0.502	0.502
5.0E-1	0.335	0.352	0.390	0.524	0.610	0.577
7.5E-1	0.418	0.389	0.505	0.544	0.640	0.656
1.0E 0	0.439	0.402	0.476	0.570	0.615	0.650
1.5E 0	0.435	0.360	0.444	0.520	0.565	0.615
2.0E 0	0.424	0.410	0.405	0.494	0.530	0.570
5.0E 0	0.426	0.424	0.280	0.351	0.419	0.422
1.0E 1	0.456	0.556	0.326	0.268	0.426	0.419
2.0E 1	0.565	0.673	0.830	0.515	0.560	0.440

TABLE IIA (contd.)

Values of $a(\lambda, t^)$*

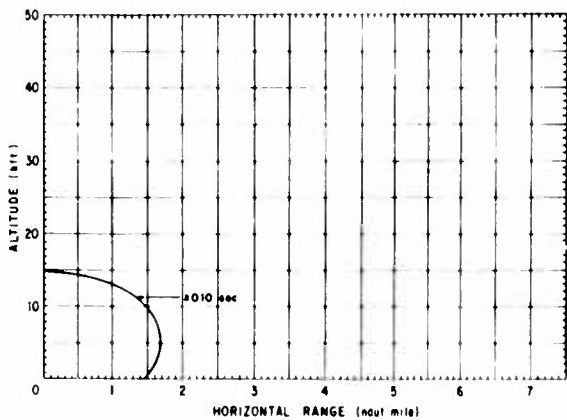
t^*	$\lambda(\mu)$				$\int b(\lambda, t^*) d\lambda$
	0.900	1.040	1.280	1.600	
5.0E-4	0.891	0.861	0.791	0.769	0.769
7.5E-4	0.771	0.859	0.786	0.769	0.656
1.0E-3	0.713	0.820	0.745	0.761	0.562
2.0E-3	0.608	0.760	0.681	0.711	0.454
2.2E-3	0.623	0.752	0.674	0.685	0.447
5.0E-3	0.636	0.682	0.615	0.606	0.438
7.5E-3	0.615	0.650	0.595	0.575	0.442
1.0E-2	0.623	0.640	0.595	0.545	0.445
2.0E-2	0.620	0.636	0.574	0.520	0.459
5.0E-2	0.565	0.523	0.520	0.481	0.431
7.5E-2	0.547	0.451	0.460	0.481	0.420
1.0E-1	0.535	0.501	0.430	0.477	0.419
2.0E-1	0.540	0.510	0.475	0.401	0.473
5.0E-1	0.532	0.656	0.633	0.388	0.535
7.5E-1	0.682	0.638	0.624	0.448	0.550
1.0E 0	0.615	0.611	0.594	0.401	0.550
1.5E 0	0.595	0.586	0.549	0.388	0.527
2.0E 0	0.545	0.561	0.542	0.401	0.502
5.0E 0	0.435	0.426	0.426	0.397	0.388
1.0E 1	0.376	0.419	0.405	0.394	0.354
2.0E 1	0.397	0.464	0.444	0.373	0.324

APPENDIX B

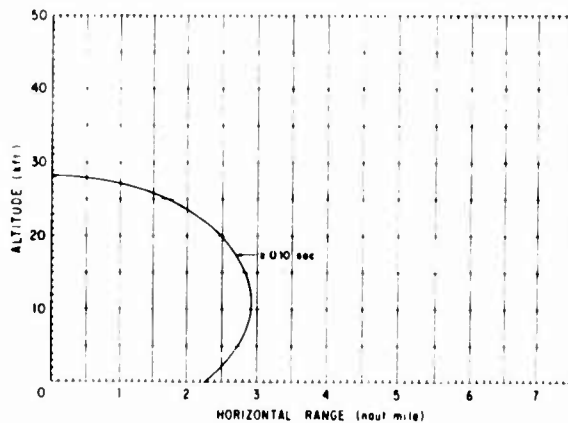
SAFE SEPARATION DISTANCE CURVES FOR RETINAL BURNS

Safe separation distances for retinal burns have been calculated by the method described in this report for seven yields (0.01, 0.10, 1.0, 10, 100, 1,000, and 10,000 KT), three burst heights (1.0, 10, and 50 kft.), two visibilities (10 and 100 km.), and for day and night conditions. The results of these calculations are included in this appendix. Each graph presents safe separation distance as a function of observer altitude for a particular yield, burst height, visibility, and for day or night conditions. Blink time is the parameter between curves, and blink times of 0.10, 0.15, 0.20, 0.50, 1.0, and 5.0 sec. are included in each group except where interpolation between times is obvious, as in the case of very closely spaced curves.

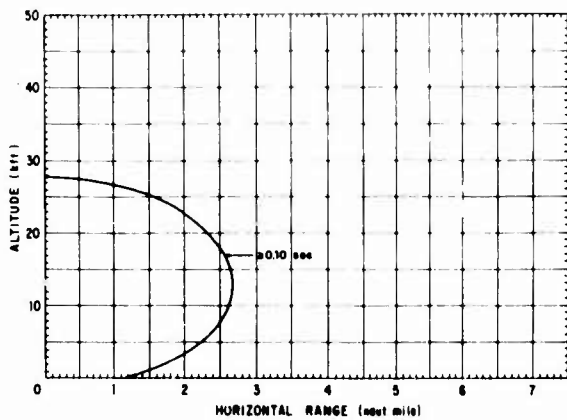
All graphs for day conditions are presented first (figs. 1B-38B) and are followed by those for night conditions (figs. 39B-76B). Within these large divisions, the graphs are arranged in the order of increasing yield; a further subdivision is made for increasing burst heights. For burst heights of 50 kft. the safe separation distances should be used with caution.



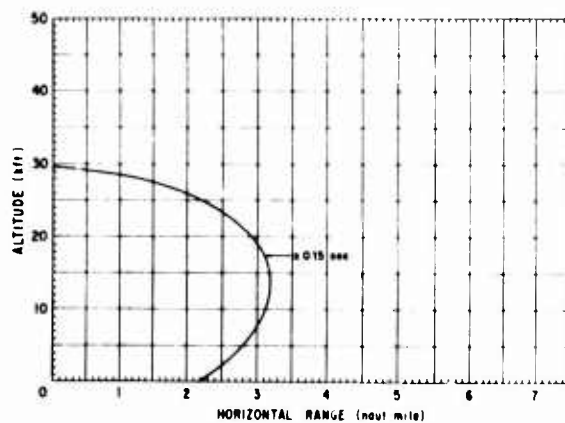
1B—Blink time, 0.1 sec. or more; 0.01-KT detonation at 1,000 ft.; day; 10-km. visibility.



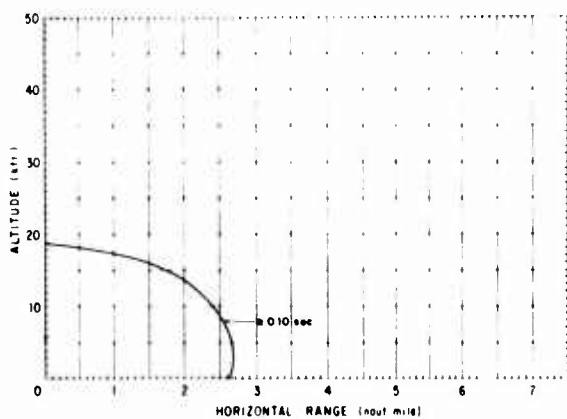
4B—Blink time, 0.1 sec. or more; 0.01-KT detonation at 10,000 ft.; day; 100-km. visibility.



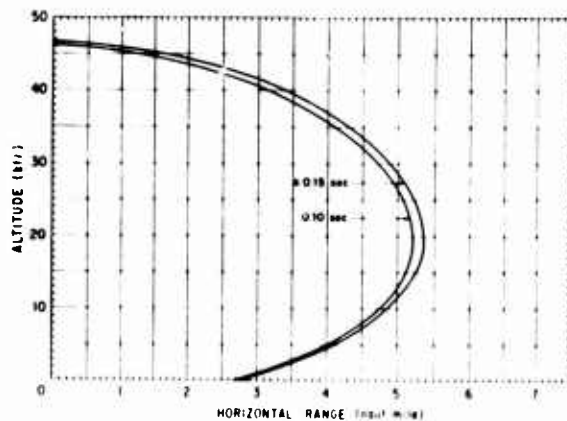
2B—Blink time, 0.1 sec. or more; 0.01-KT detonation at 10,000 ft.; day; 10-km. visibility.



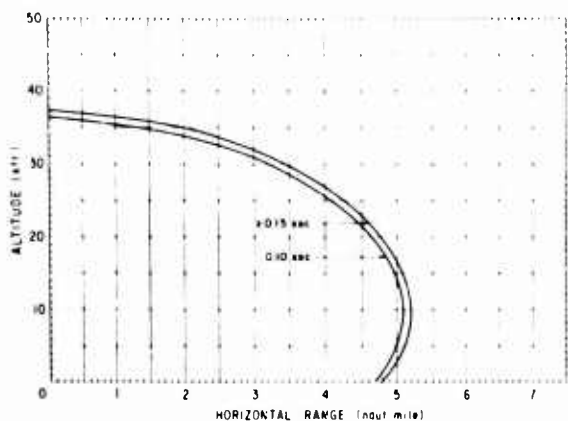
5B—Blink time, 0.15 sec. or more; 0.1-KT detonation at 1,000 ft.; day; 10-km. visibility.



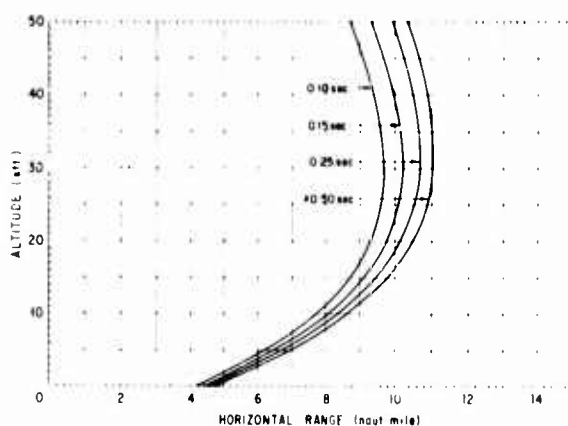
3B—Blink time, 0.1 sec. or more; 0.01-KT detonation at 1,000 ft.; day; 100-km. visibility.



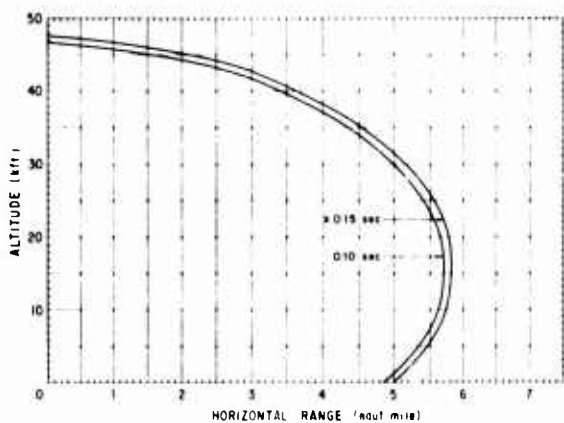
6B—Blink times, 0.1 and 0.15 sec. or more; 0.1-KT detonation at 10,000 ft.; day; 10-km. visibility.



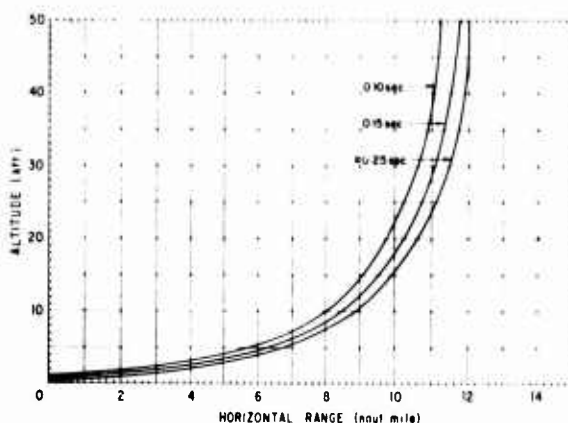
7B—Blink times, 0.1 and 0.15 sec. or more; 0.1-KT detonation at 1,000 ft.; day; 100-km. visibility.



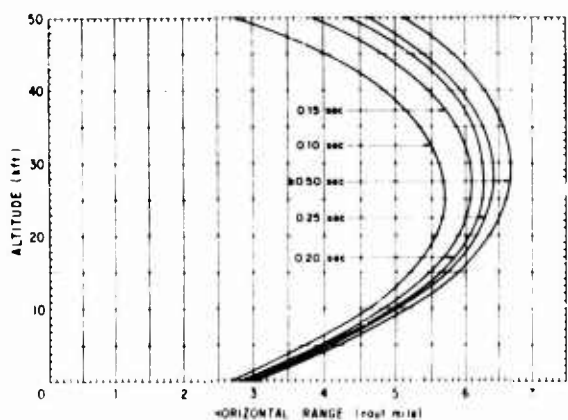
10B—Various blink times; 1-KT detonation at 10,000 ft.; day 10-km. visibility.



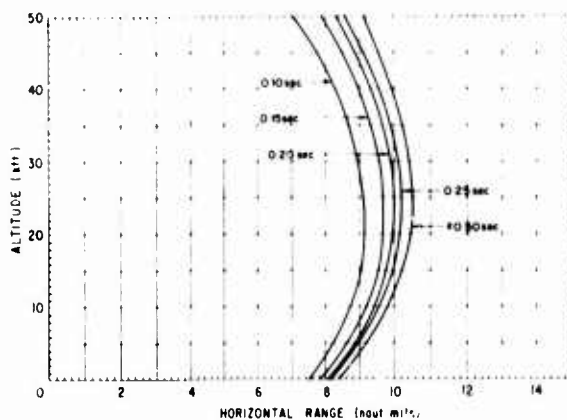
8B—Blink times, 0.1 and 0.15 sec. or more; 0.1-KT detonation at 10,000 ft.; day; 100-km. visibility.



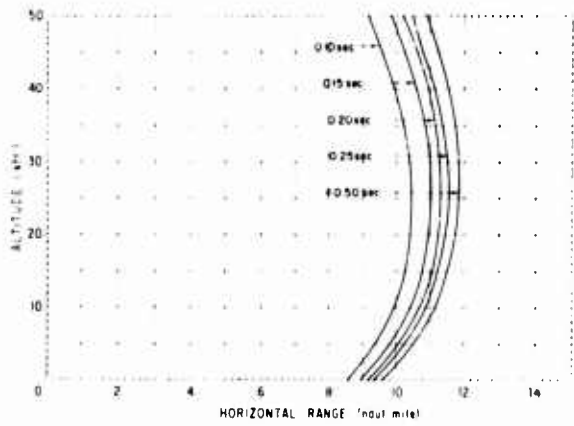
11B—Various blink times; 1-KT detonation at 50,000 ft.; day; 10-km. visibility.



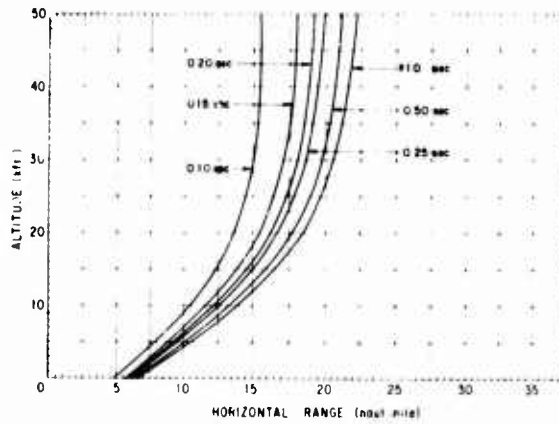
9B—Various blink times; 1-KT detonation at 1,000 ft.; day; 10-km. visibility.



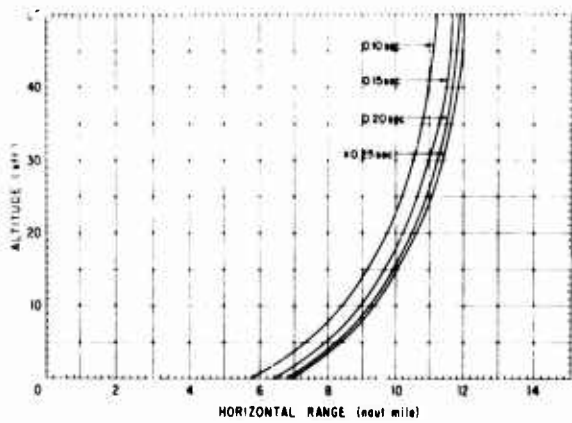
12B—Various blink times; 1-KT detonation at 1,000 ft.; day; 100-km. visibility.



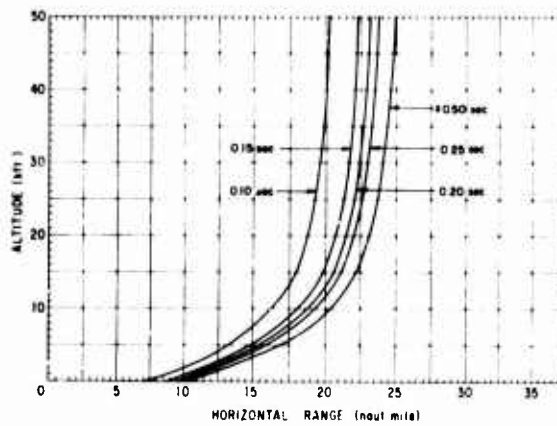
13B—Various blink times; 1-KT detonation at 10,000 ft.; day; 100-km. visibility.



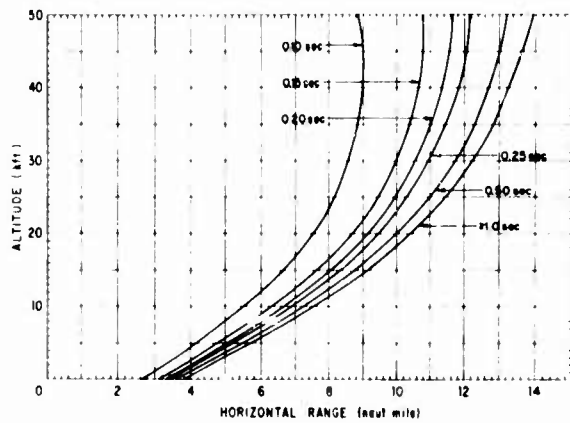
16B—Various blink times; 10-KT detonation at 10,000 ft.; day; 10-km. visibility.



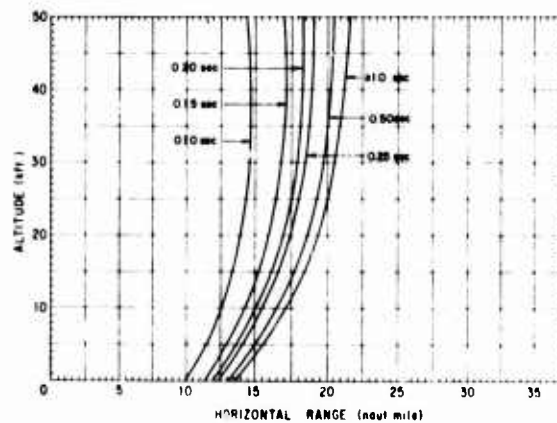
14B—Various blink times; 1-KT detonation at 50,000 ft.; day; 100-km. visibility.



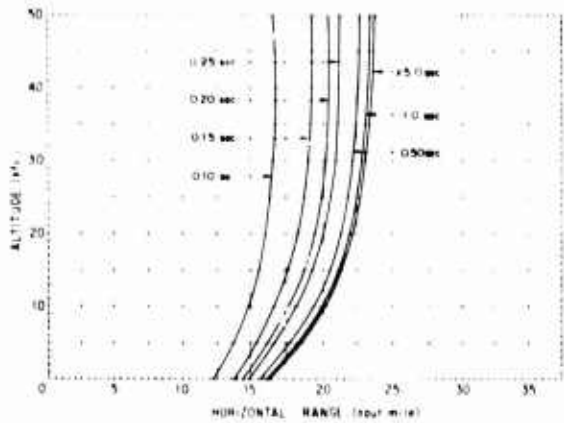
17B—Various blink times; 10-KT detonation at 50,000 ft.; day; 10-km. visibility.



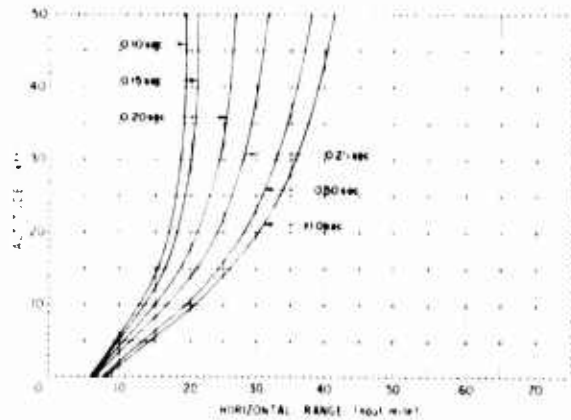
15B—Various blink times; 10-KT detonation at 1,000 ft.; day; 10-km. visibility.



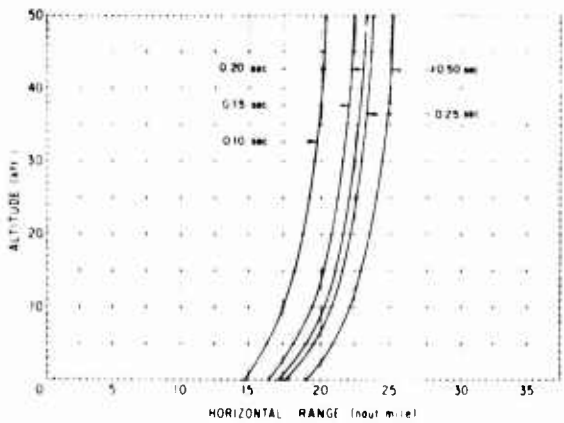
18B—Various blink times; 10-KT detonation at 1,000 ft.; day; 100-km. visibility.



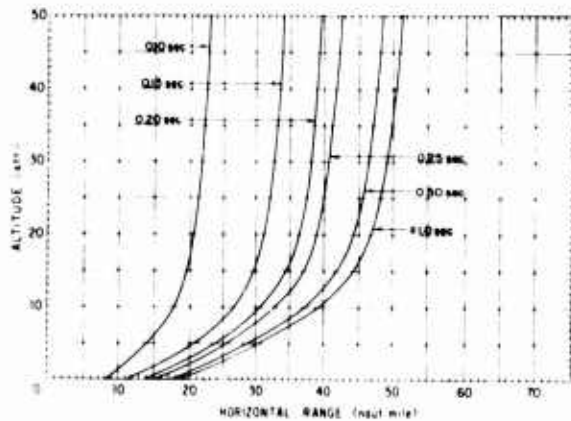
19B—Various blink times; 10-KT detonation at 10,000 ft.; day; 100-km. visibility



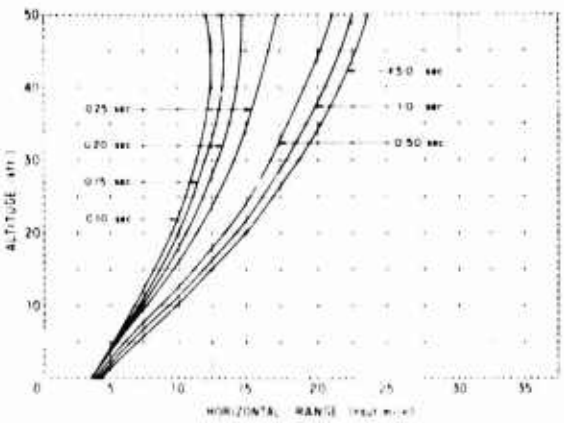
22B—Various blink times; 100-KT detonation at 10,000 ft.; day; 10-km. visibility.



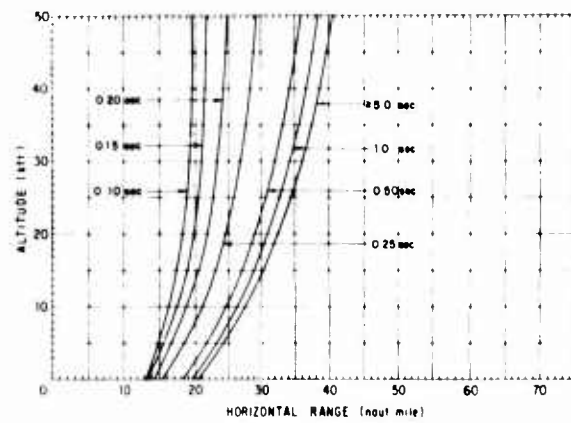
20B—Various blink times; 10-KT detonation at 50,000 ft.; day; 100-km. visibility.



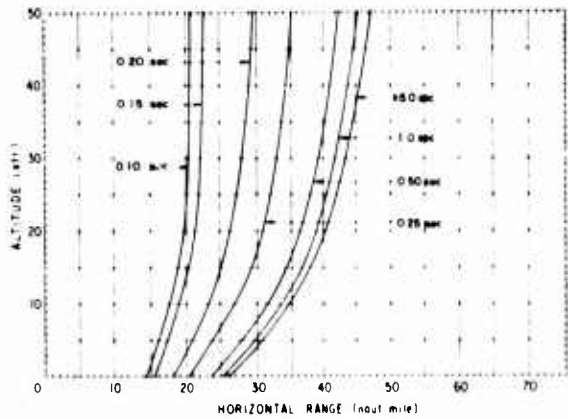
23B—Various blink times; 100-KT detonation at 50,000 ft.; day; 10-km. visibility.



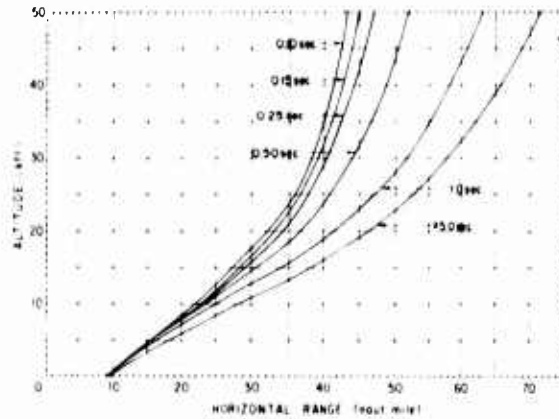
21B—Various blink times; 100-KT detonation at 1,000 ft.; day; 10-km. visibility.



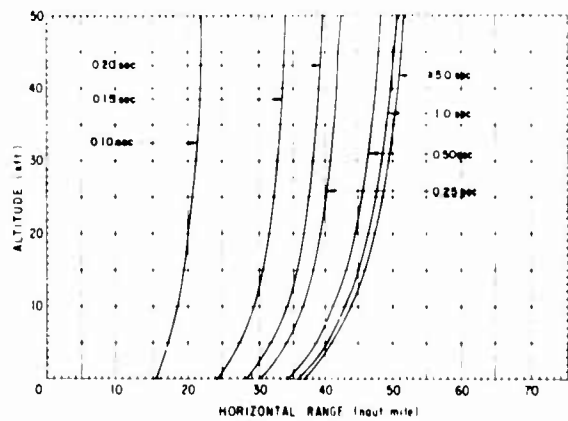
24B—Various blink times; 100-KT detonation at 1,000 ft.; day; 100-km. visibility.



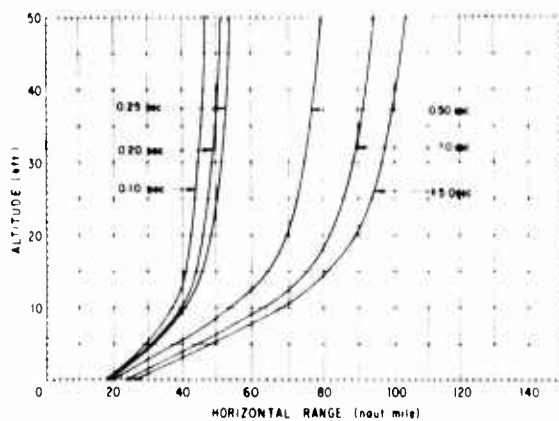
25B—Various blink times; 100-kT detonation at 10,000 ft.; day; 100-km. visibility.



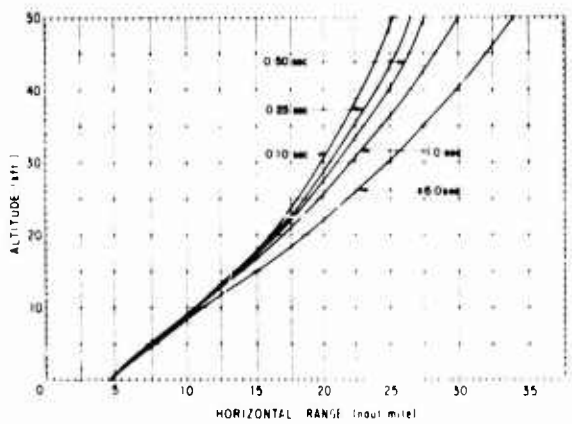
26B—Various blink times; 1,000-KT detonation at 10,000 ft.; day; 10-km. visibility.



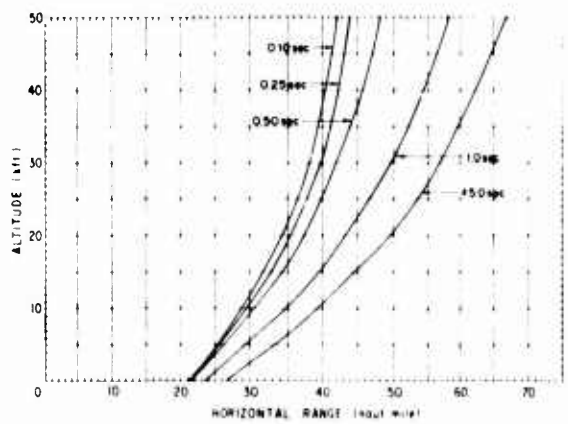
27B—Various blink times; 100-KT detonation at 50,000 ft.; day; 100-km. visibility.



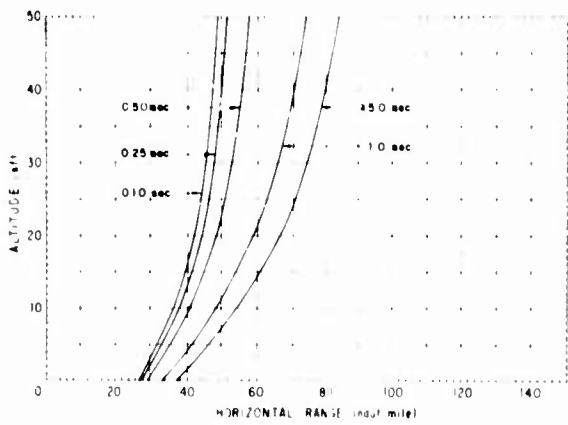
28B—Various blink times; 1,000-KT detonation at 50,000 ft.; day; 10-km. visibility.



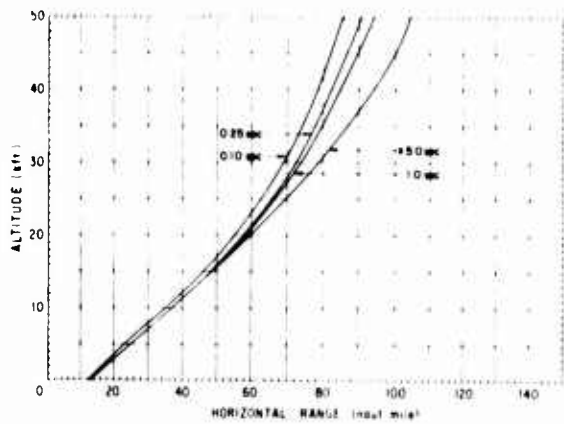
29B—Various blink times; 1,000-KT detonation at 1,000 ft.; day; 10-km. visibility.



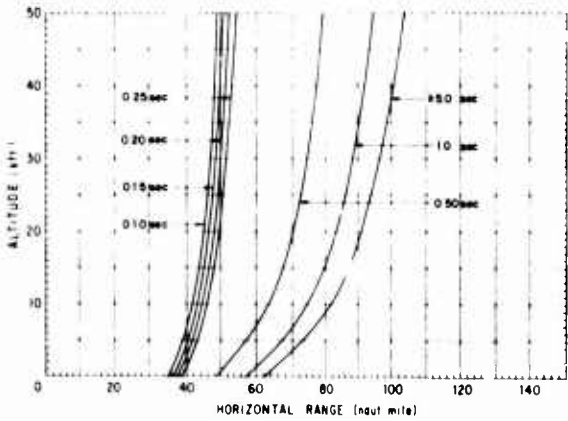
30B—Various blink times; 1,000-KT detonation at 1,000 ft.; day; 100-km. visibility.



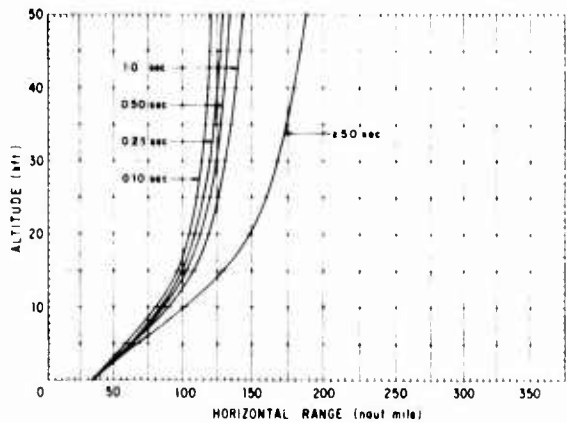
31B—Various blink times; 1,000-KT detonation at 10,000 ft.; day; 100-km. visibility.



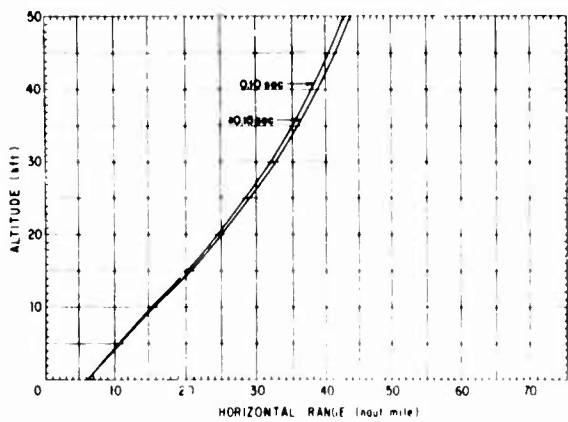
34B—Various blink times; 10,000-KT detonation at 10,000 ft.; day; 10-km. visibility.



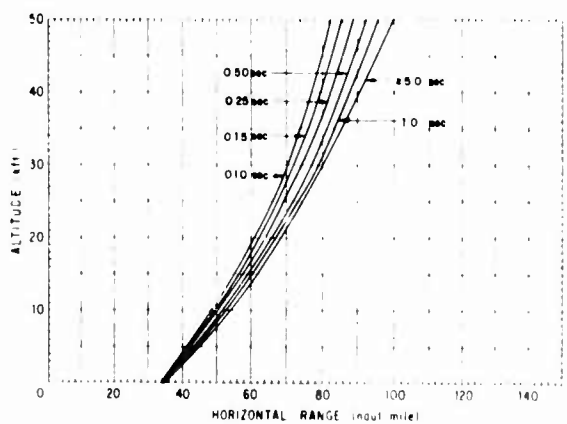
32B—Various blink times; 1,000-KT detonation at 50,000 ft.; day; 100-km. visibility.



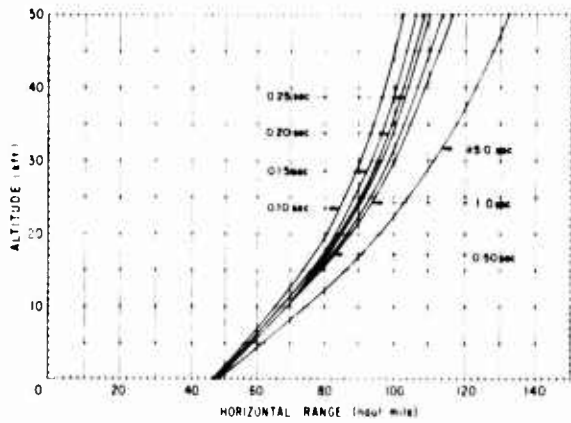
35B—Various blink times; 10,000-KT detonation at 50,000 ft.; day; 10-km. visibility.



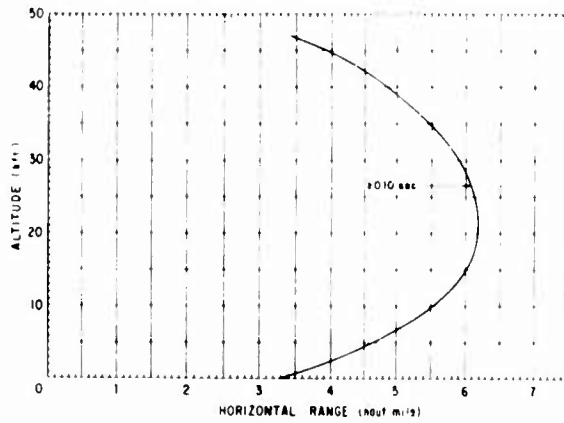
33B—Blink times, 0.1 and 0.15 sec. or more; 10,000-KT detonation at 1,000 ft.; day; 10-km. visibility.



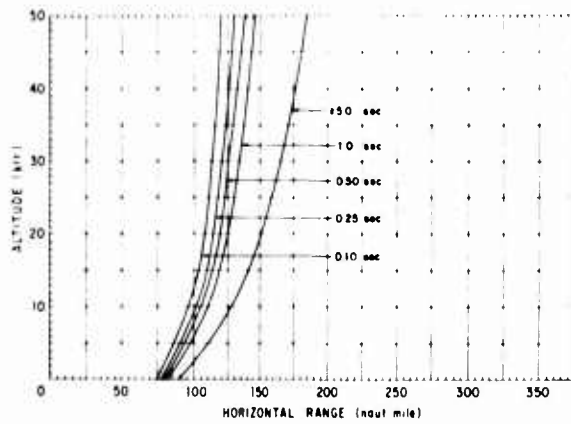
36B—Various blink times; 10,000-KT detonation at 1,000 ft.; day; 100-km. visibility.



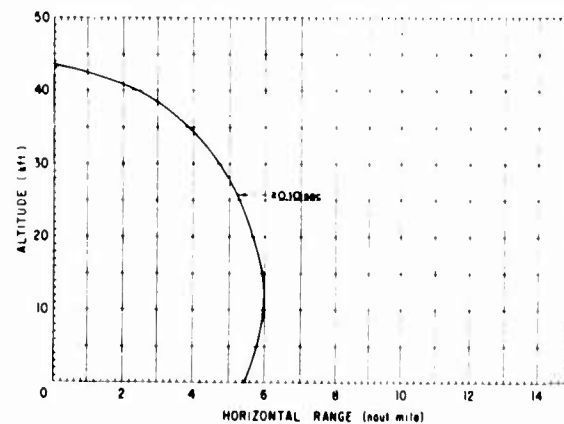
37B—Various blink times; 10,000-KT detonation at 10,000 ft.; day; 100-km. visibility.



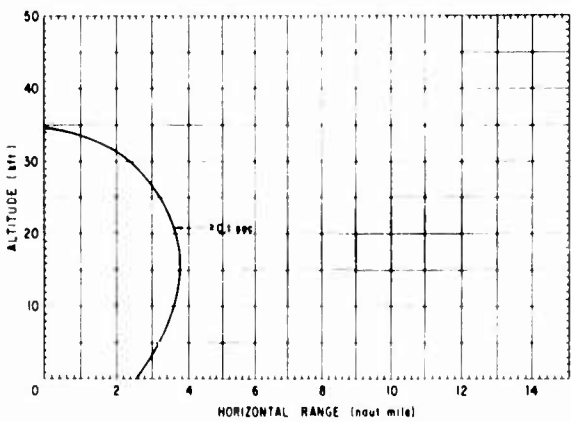
40B—Blink time, 0.1 sec. or more; 0.01-KT detonation at 10,000 ft.; night; 10-km. visibility.



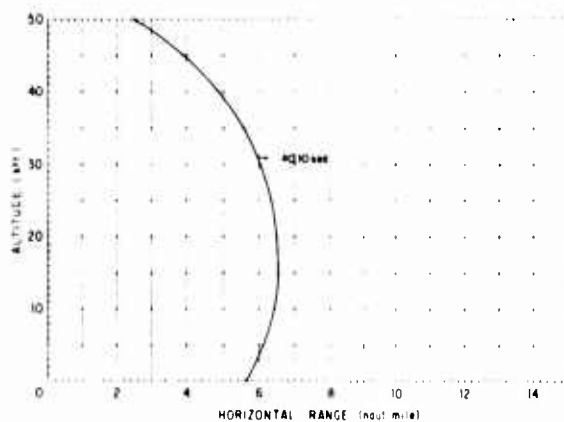
38B—Various blink times; 10,000-KT detonation at 50,000 ft.; day; 100-km. visibility.



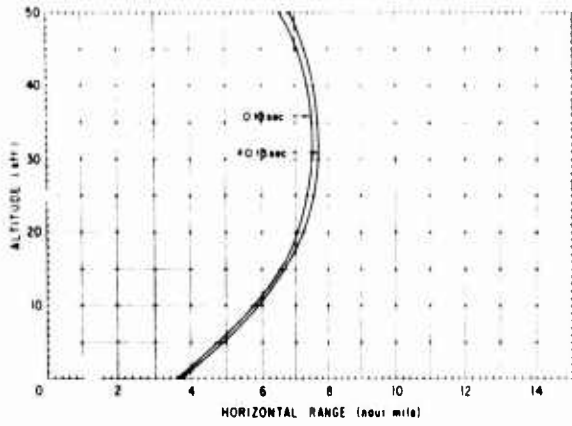
41B—Blink time, 0.1 sec. or more; 0.01-KT detonation at 1,000 ft.; night; 100-km. visibility.



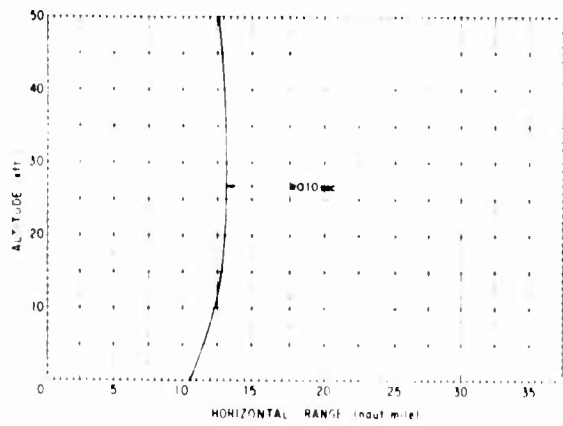
39B—Blink time, 0.1 sec. or more; 0.01-KT detonation at 1,000 ft.; night; 10-km. visibility.



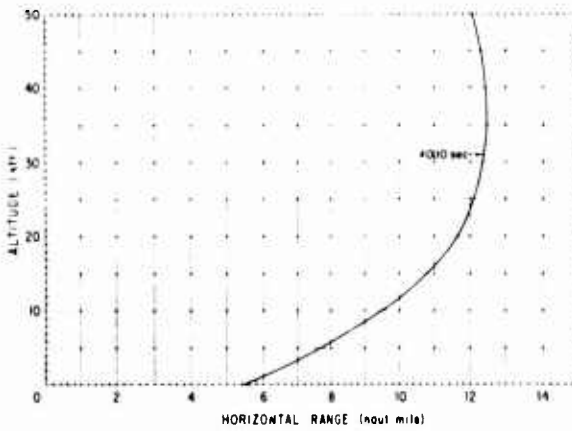
42B—Blink time, 0.1 sec. or more; 0.01-KT detonation at 10,000 ft.; night; 100-km. visibility.



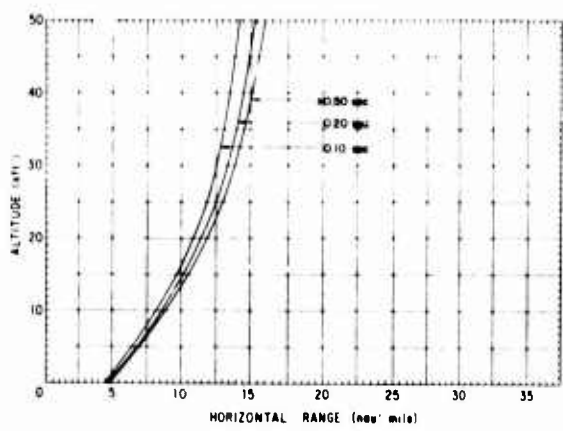
43B—Blink times, 0.1 and 0.15 sec. or more; 0.1-KT detonation at 1,000 ft.; night; 10-km. visibility.



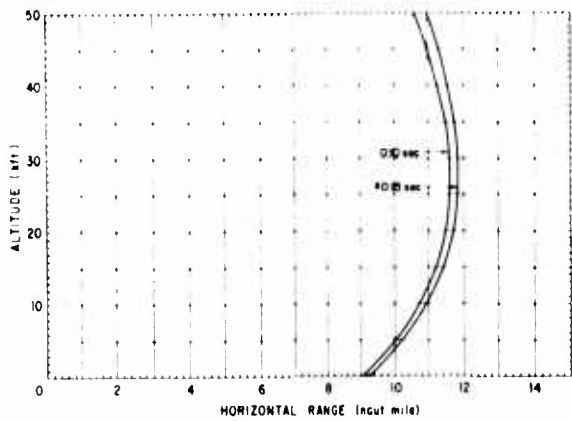
46B—Blink time, 0.1 sec. or more; 0.1-KT detonation at 10,000 ft.; night; 100-km. visibility.



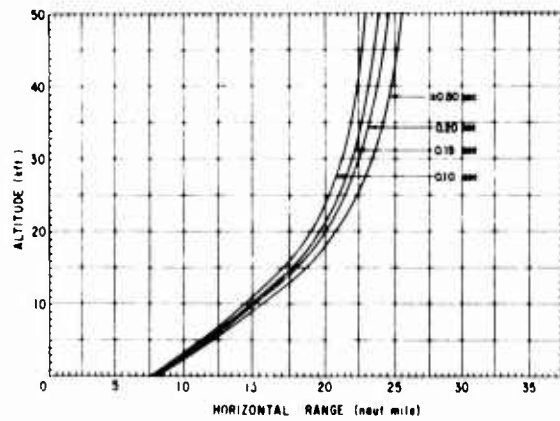
44B—Blink time, 0.1 sec. or more; 0.1-KT detonation at 10,000 ft.; night; 10-km. visibility.



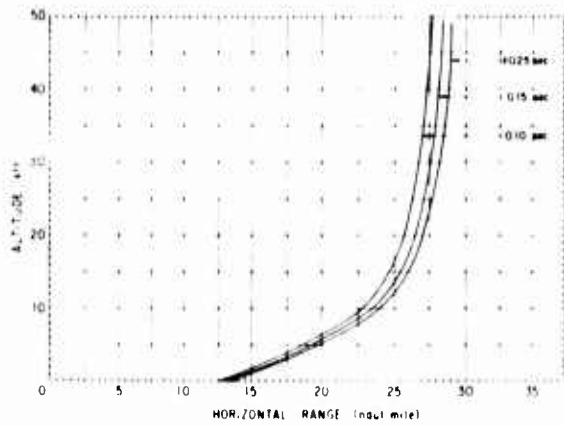
47B—Various blink times; 1-KT detonation at 1,000 ft.; night; 10-km. visibility.



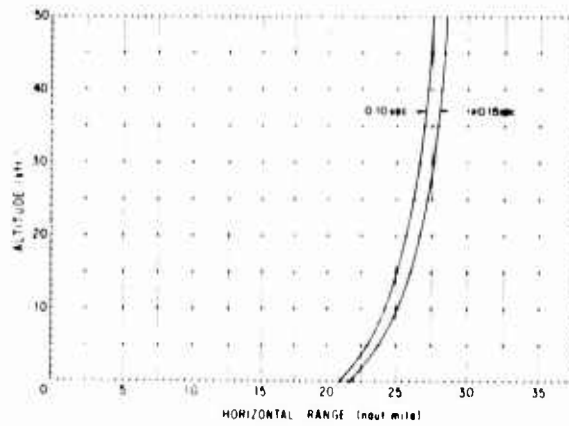
45B—Blink times, 0.1 and 0.15 sec. or more; 0.1-KT detonation at 1,000 ft.; night; 100-km. visibility.



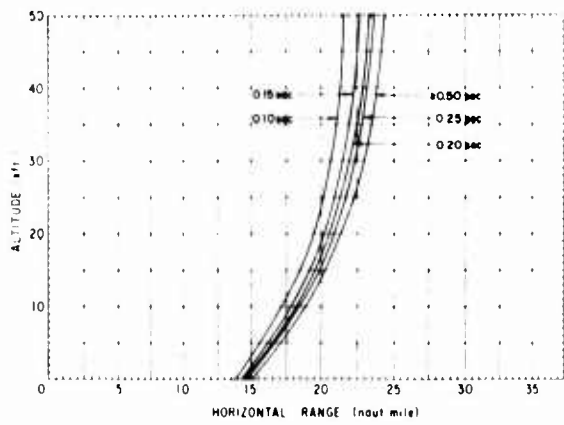
48B—Various blink times; 1-KT detonation at 10,000 ft.; night; 10-km. visibility.



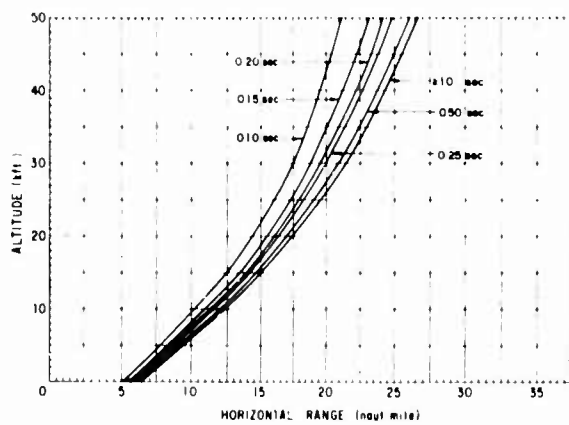
49B—Various blink times; 1-KT detonation at 50,000 ft.; night; 10-km. visibility.



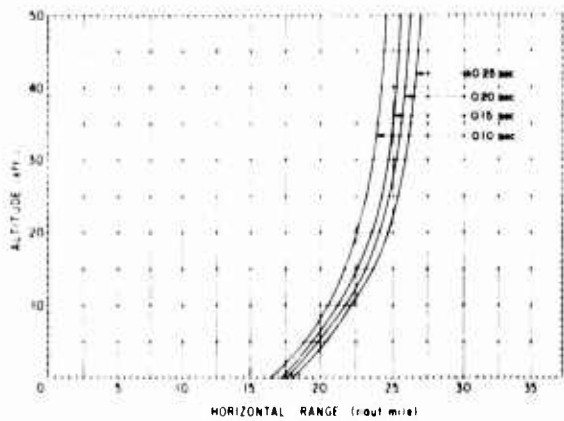
52B—Blink times, 0.1 and 0.15 sec. or more; 1-KT detonation at 50,000 ft.; night; 100-km. visibility.



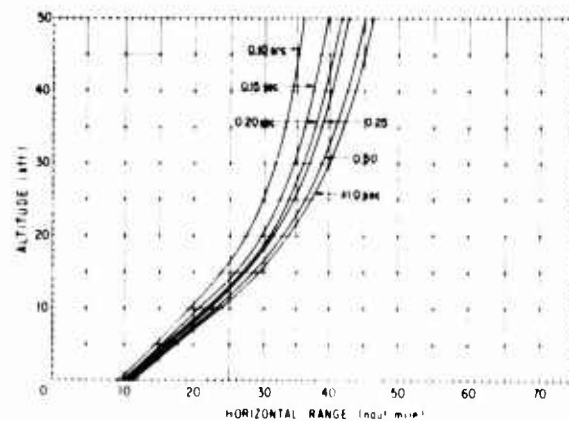
50B—Various blink times; 1-KT detonation at 1,000 ft.; night; 100-km. visibility.



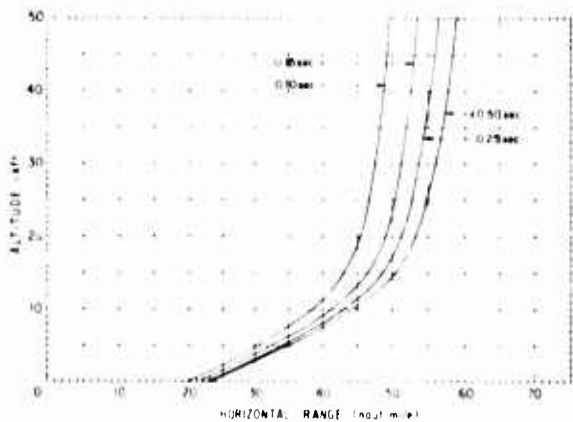
53B—Various blink times; 10-KT detonation at 1,000 ft.; night; 10-km. visibility.



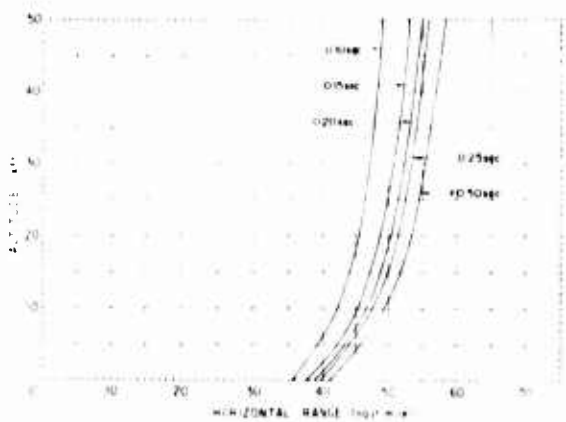
51B—Various blink times; 1-KT detonation at 10,000 ft.; night; 100-km. visibility.



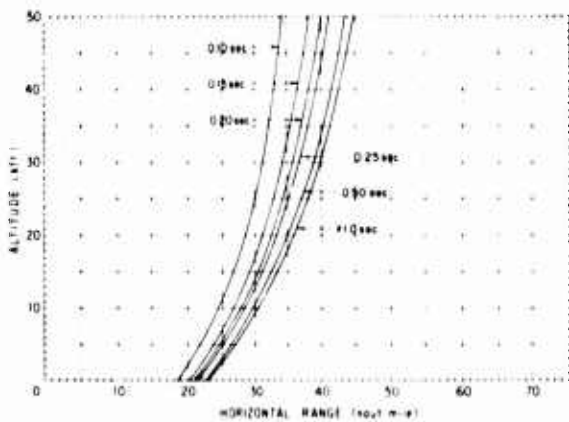
54B—Various blink times; 10-KT detonation at 10,000 ft.; night; 10-km. visibility.



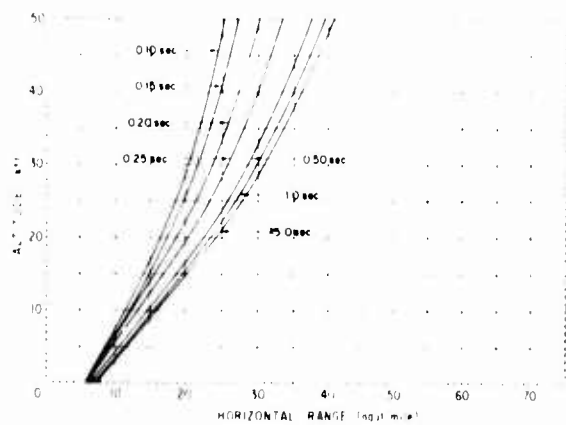
55B—Various blink times; 10-KT detonation at 50,000 ft.; night; 10-km. visibility.



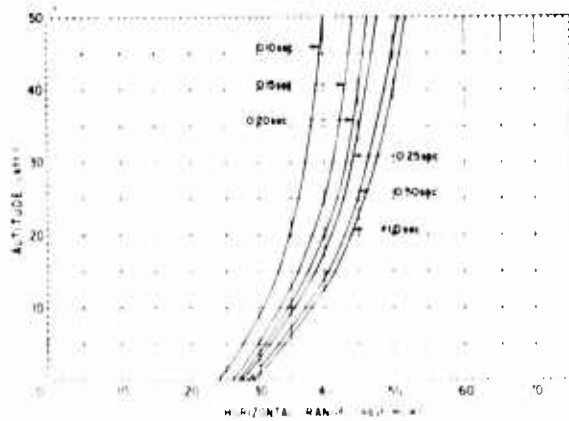
58B—Various blink times; 10-KT detonation at 50,000 ft.; night; 100-km. visibility.



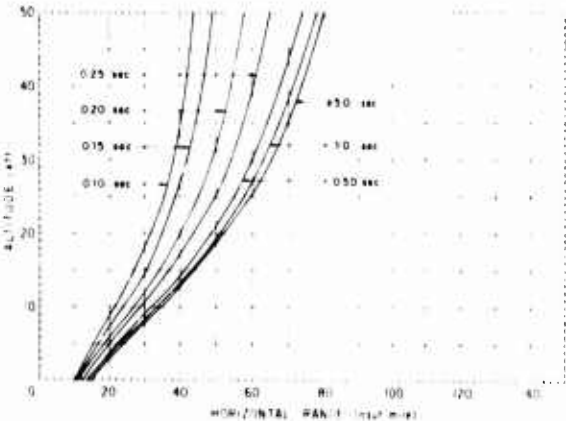
56B—Various blink times; 10-KT detonation at 1,000 ft.; night; 100-km. visibility.



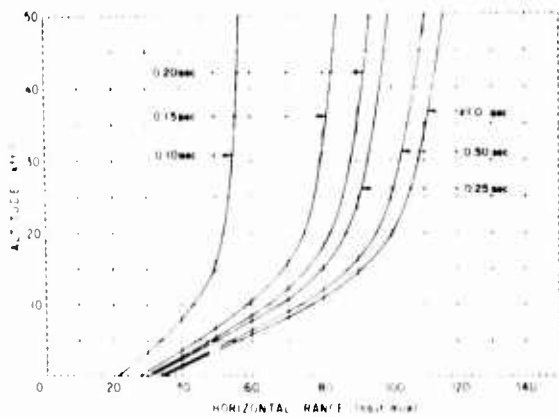
59B—Various blink times; 100-KT detonation at 1,000 ft.; night; 10-km. visibility.



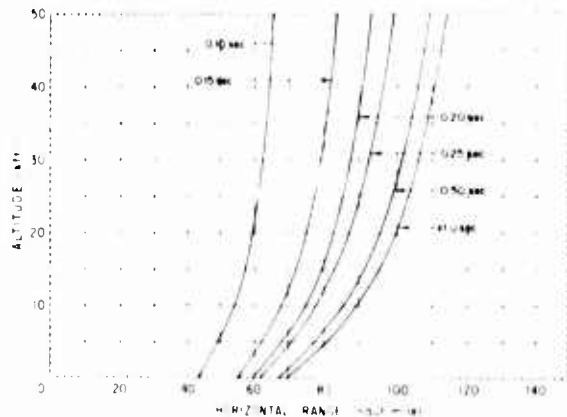
57B—Various blink times; 10-KT detonation at 10,000 ft.; night; 100-km. visibility.



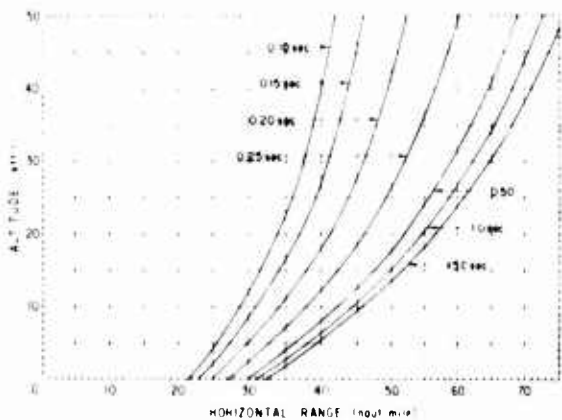
60B—Various blink times; 100-KT detonation at 10,000 ft.; night; 10-km. visibility.



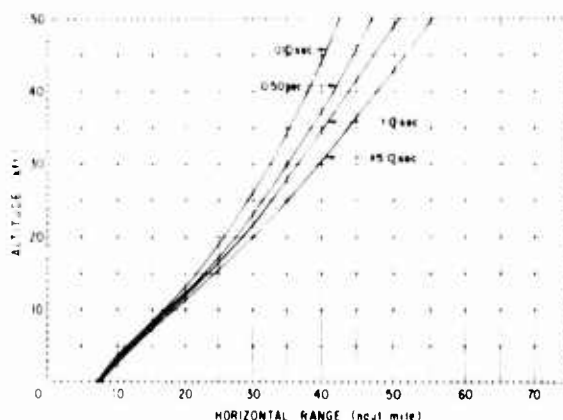
61B—Various blink times; 100-KT detonation at 50,000 ft.; night; 10-km. visibility.



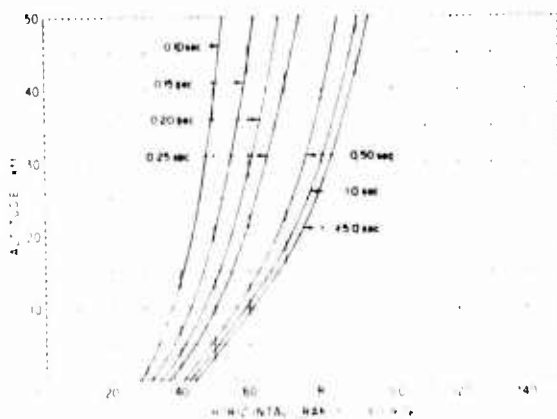
64B—Various blink times; 100-KT detonation at 50,000 ft.; night; 100-km. visibility.



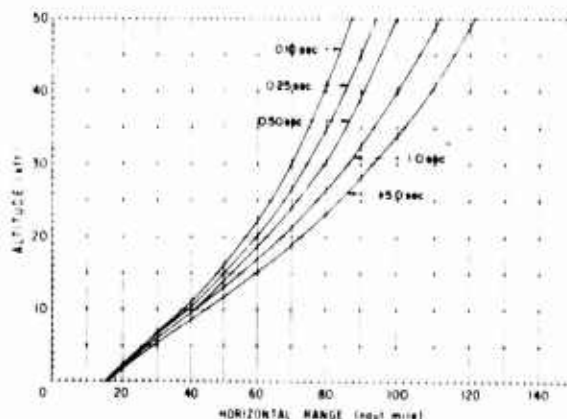
62B—Various blink times; 100-KT detonation at 1,000 ft.; night; 100-km. visibility.



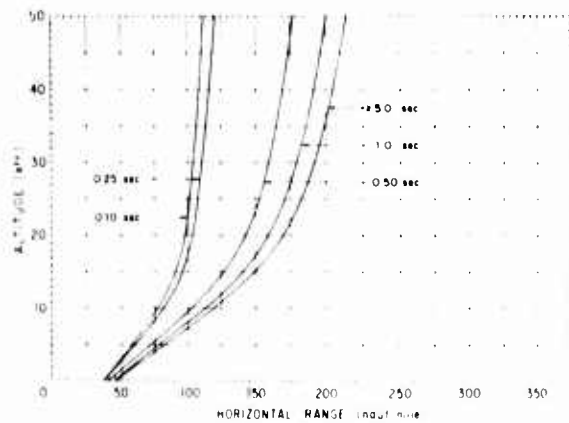
65B—Various blink times; 1,000-KT detonation at 1,000 ft.; night; 10-km. visibility.



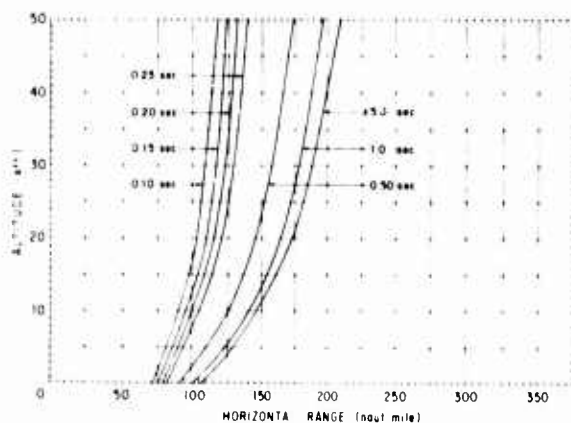
63B—Various blink times; 100-KT detonation at 10,000 ft.; night; 100-km. visibility.



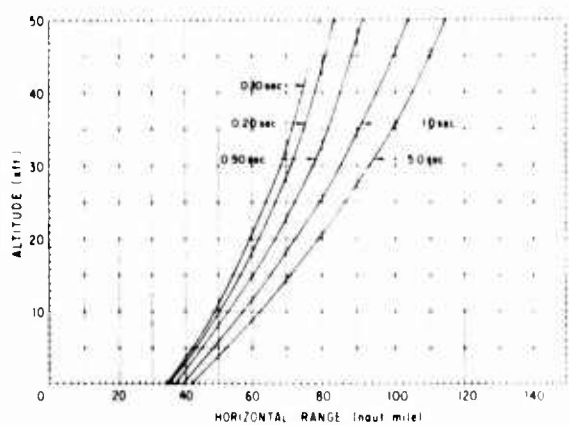
66B—Various blink times; 1,000-KT detonation at 10,000 ft.; night; 10-km. visibility.



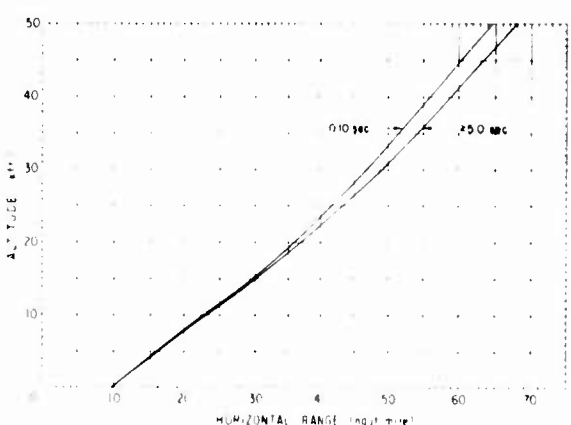
67B—Various blink times; 1,000-KT detonation at 50,000 ft.; night; 10-km. visibility.



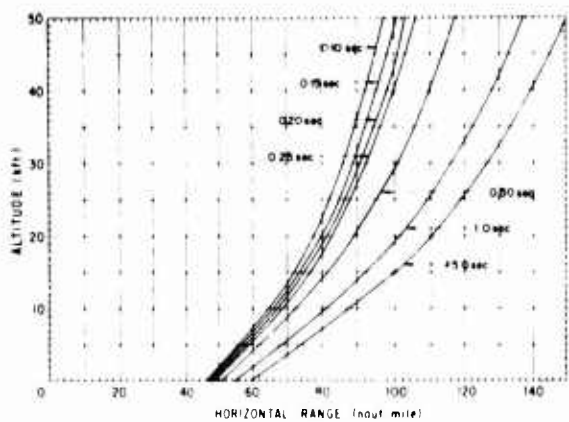
70B—Various blink times; 1,000-KT detonation at 50,000 ft.; night; 100-km. visibility.



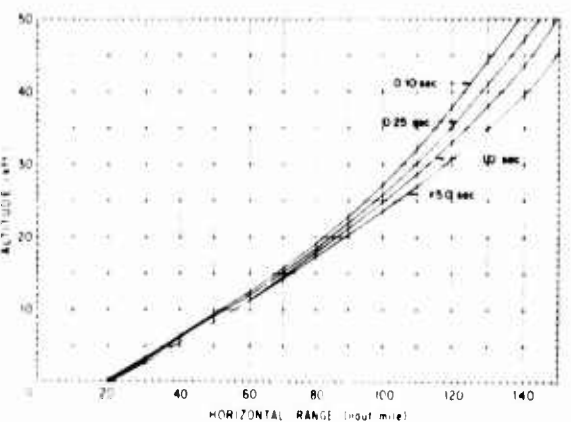
68B—Various blink times; 1,000-KT detonation at 1,000 ft.; night; 100-km. visibility.



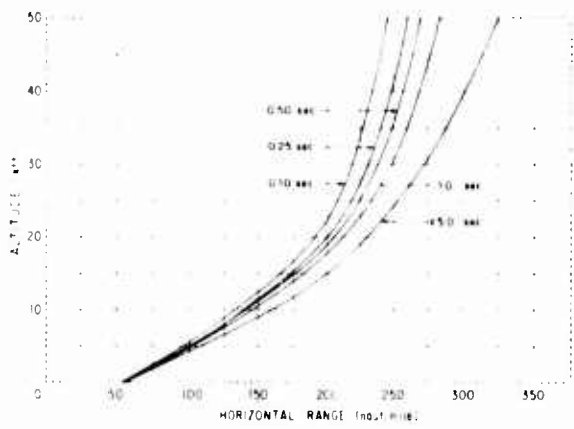
71B—Blink times, 0.1 and 5 sec. or more; 10,000-KT detonation at 1,000 ft.; night; 10-km. visibility.



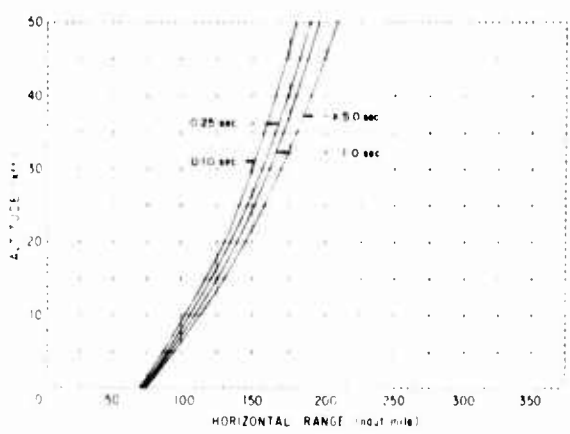
69B—Various blink times; 1,000-KT detonation at 10,000 ft.; night; 100-km. visibility.



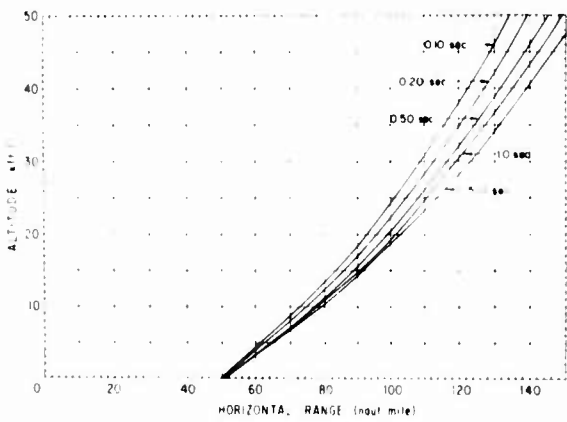
72B—Various blink times; 10,000-KT detonation at 10,000 ft.; night; 10-km. visibility.



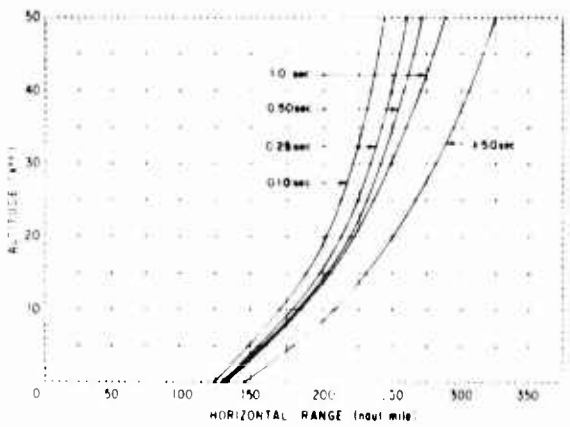
73B—Various blink times; 10,000-KT detonation at 60,000 ft.; night; 10-km. visibility.



75B—Various blink times; 10,000-KT detonation at 10,000 ft.; night; 100-km. visibility.



74B—Various blink times; 10,000-KT detonation at 1,000 ft.; night; 100-km. visibility.



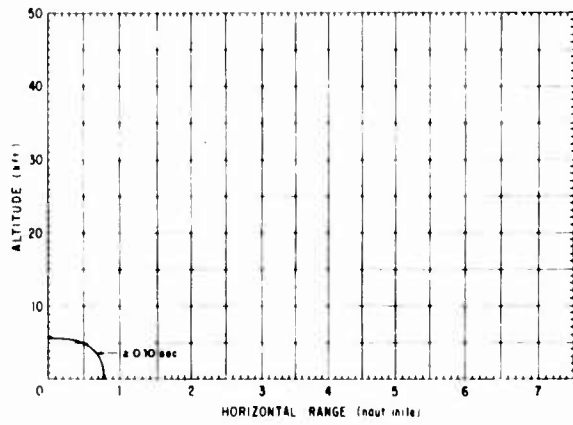
76B—Various blink times; 10,000-KT detonation at 60,000 ft.; night; 100-km. visibility.

APPENDIX C

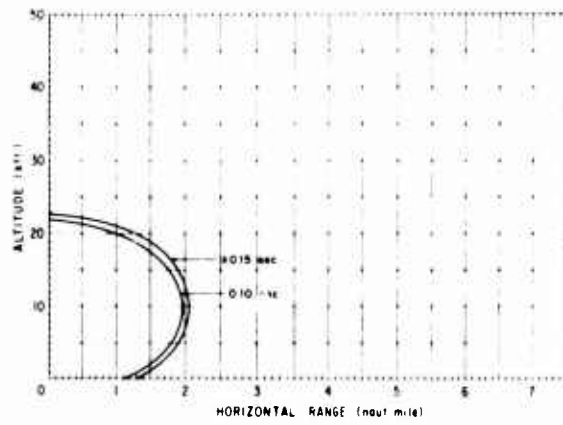
SAFE SEPARATION DISTANCE CURVES FOR FLASHBLINDNESS

Safe separation distances for flashblindness have been determined as explained in this report for seven yields (0.01, 0.10, 1.0, 10, 100, 1,000, and 10,000 KT), three burst heights (1.0, 10.0, and 50 kft.), one visibility (100 km.), and for day and night conditions. The results are presented in this appendix as a set of graphs of safe separation distance versus observer altitude. Each graph is plotted for a specified yield, burst height, visibility, and for day or night conditions, with blink time as the parameter between curves. Seven blink times (0.10, 0.15, 0.20, 0.25, 0.50, 1.0, and 5.0 sec.) are included on each graph except where the interpolation from one blink time to another is evident as in the case of closely spaced curves.

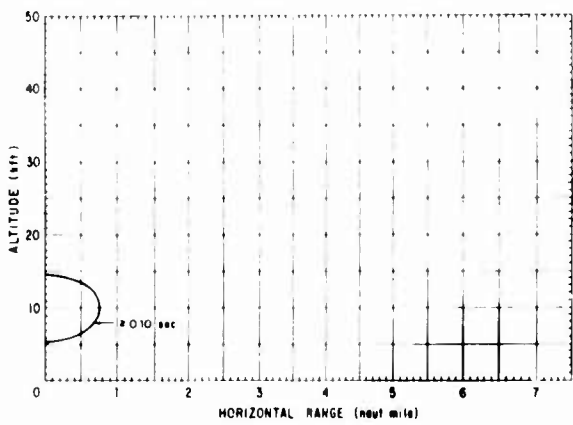
The graphs for day conditions are presented first (figs. 1C-19C) and are followed by those for night conditions (figs. 20C-38C). Each of these major divisions is then subdivided in the order of increasing yield, and a further subdivision is made for the increasing burst heights. The safe separation distances obtained from these graphs for weapons detonated at 50 kft. should be used with caution.



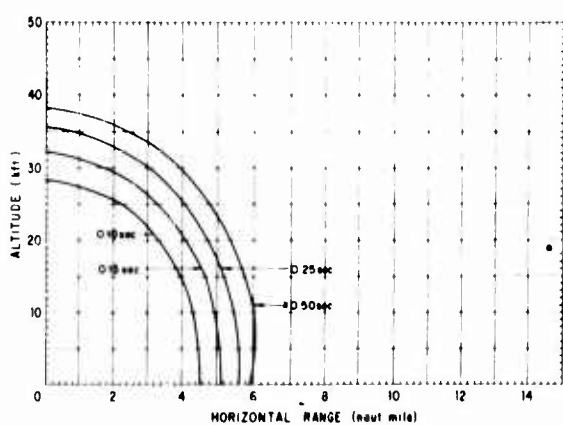
1C—Blink time, 0.1 sec. or more; 0.01-KT detonation at 1,000 ft.; day; 100-km. visibility.



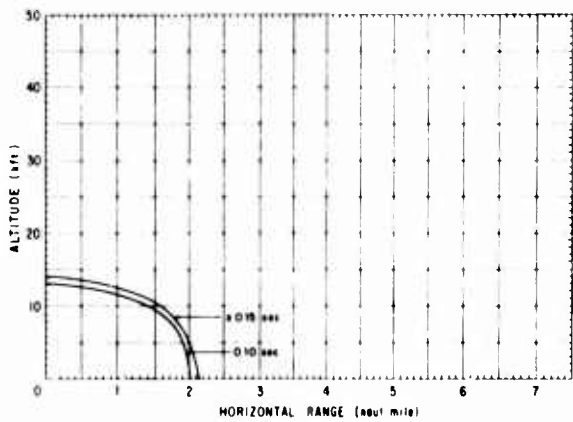
4C—Blink times, 0.1 and 0.15 sec. or more; 0.1-KT detonation at 10,000 ft.; day; 100-km. visibility.



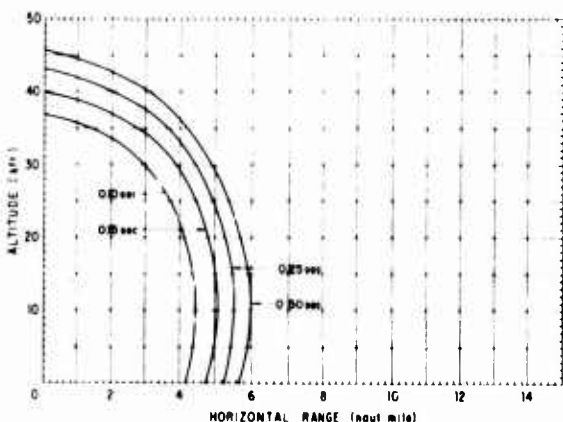
2C—Blink time, 0.1 sec. or more; 0.01-KT detonation at 10,000 ft.; day; 100-km. visibility.



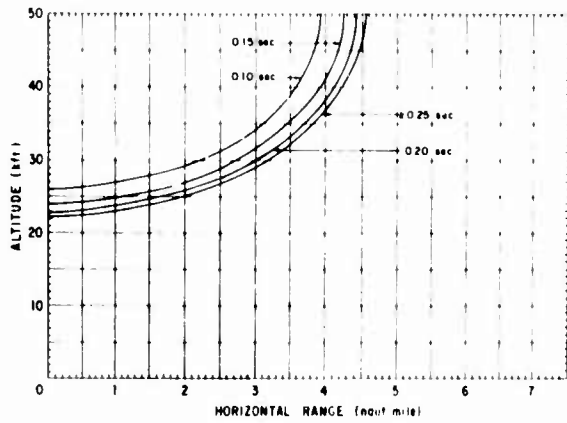
5C—Various blink times; 1-KT detonation at 1,000 ft.; day; 100-km. visibility.



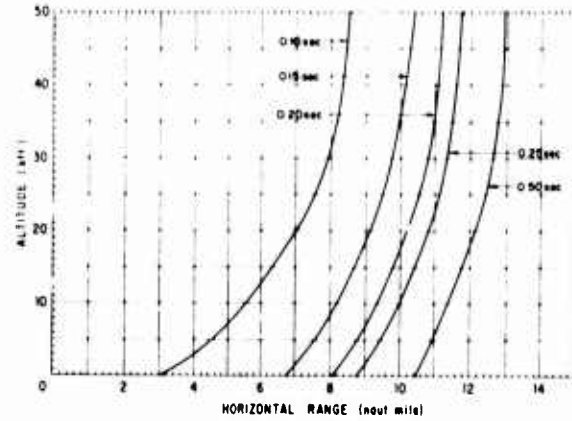
3C—Blink times, 0.1 and 0.15 sec. or more; 0.1-KT detonation at 1,000 ft.; day; 100-km. visibility.



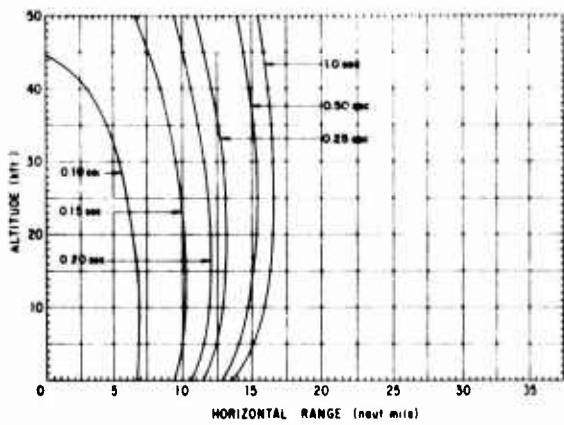
6C—Various blink times; 1-KT detonation at 10,000 ft.; day; 100-km. visibility.



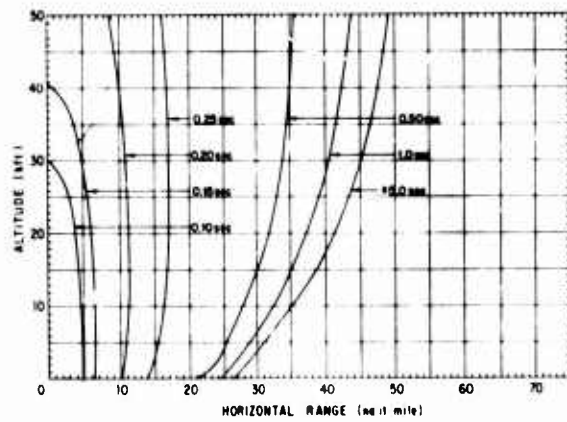
7C—Various blink times; 1-KT detonation at 50,000 ft.; day; 100-km. visibility.



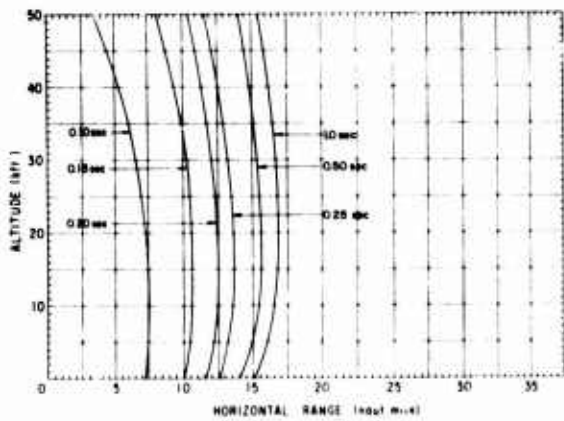
10C—Various blink times; 10-KT detonation at 50,000 ft.; day; 100-km. visibility.



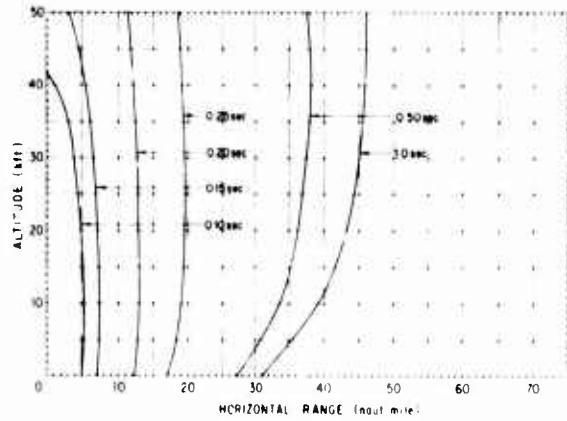
8C—Various blink times; 10-KT detonation at 1,000 ft.; day; 100-km. visibility.



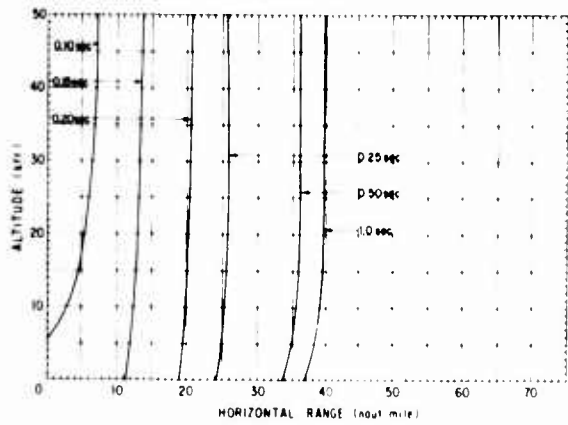
11C—Various blink times; 100-KT detonation at 1,000 ft.; day; 100-km. visibility.



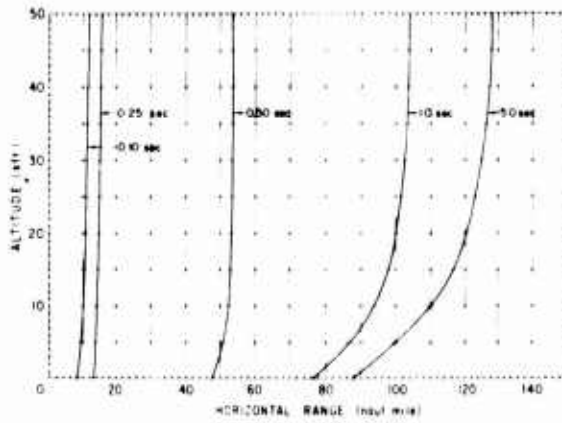
9C—Various blink times; 10-KT detonation at 10,000 ft.; day; 100-km. visibility.



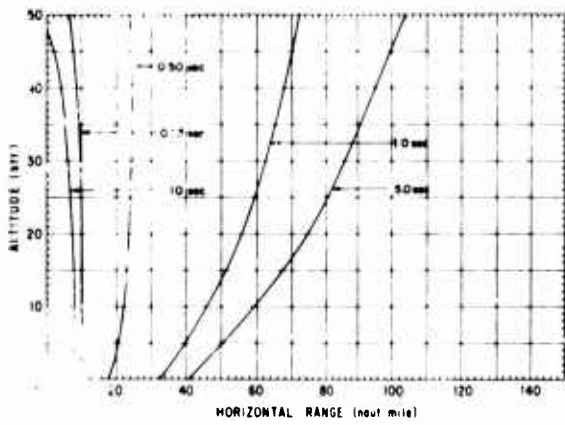
12C—Various blink times; 100-KT detonation at 10,000 ft.; day; 100-km. visibility.



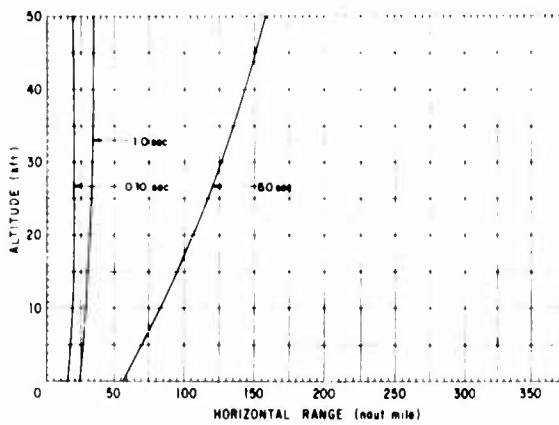
13C—Various blink times; 100-KT detonation at 50,000 ft.; day; 100-km. visibility.



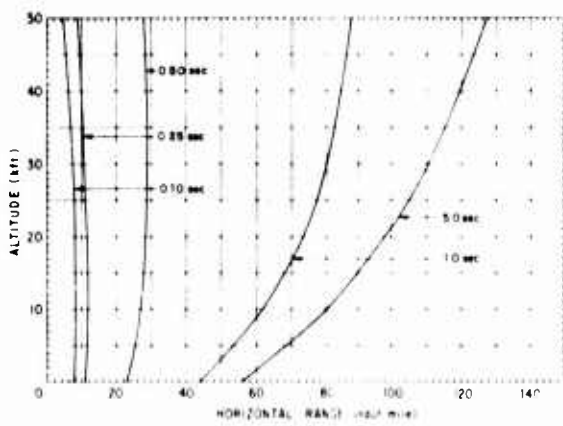
16C—Various blink times; 1,000-KT detonation at 50,000 ft.; day; 100-km. visibility.



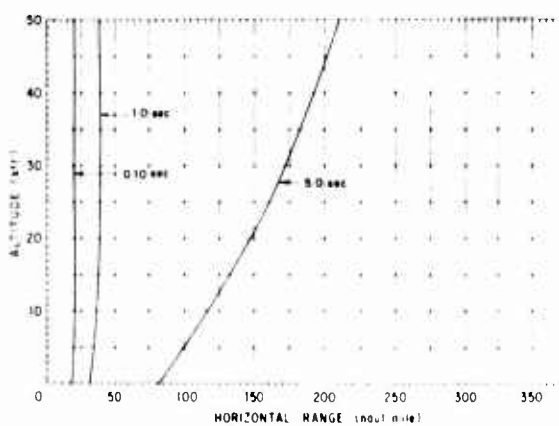
14C—Various blink times; 1,000-KT detonation at 1,000 ft.; day; 100-km. visibility.



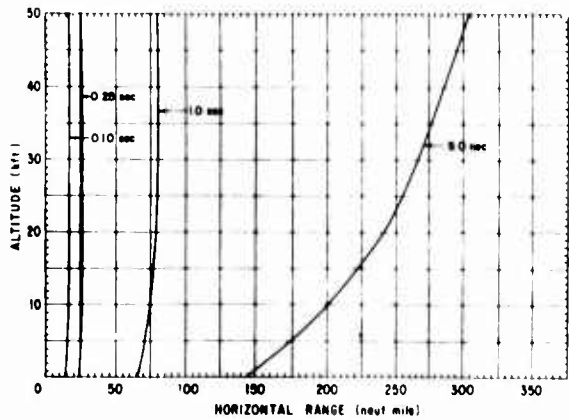
17C—Various blink times; 10,000-KT detonation at 1,000 ft.; day; 100-m. visibility.



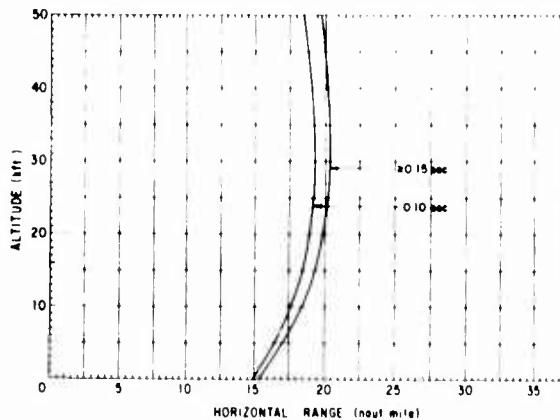
15C—Various blink times; 1,000-KT detonation at 10,000 ft.; day; 100-km. visibility.



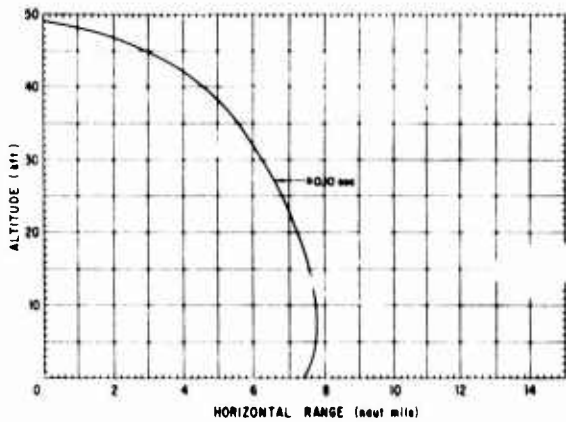
18C—Various blink times; 10,000-KT detonation at 10,000 ft.; day; 100-km. visibility.



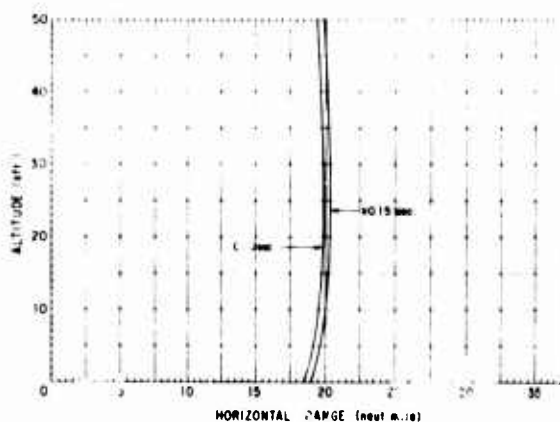
19C—Various blink times; 10,000-KT detonation at 50,000 ft.; day; 100-km. visibility.



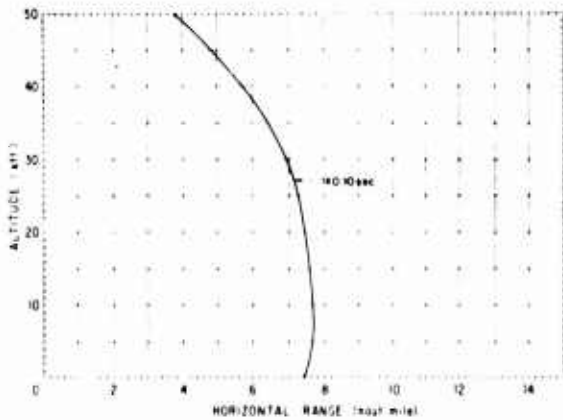
22C—Blink times, 0.1 and 0.15 sec. or more; 0.1-KT detonation at 1,000 ft.; night; 100-km. visibility.



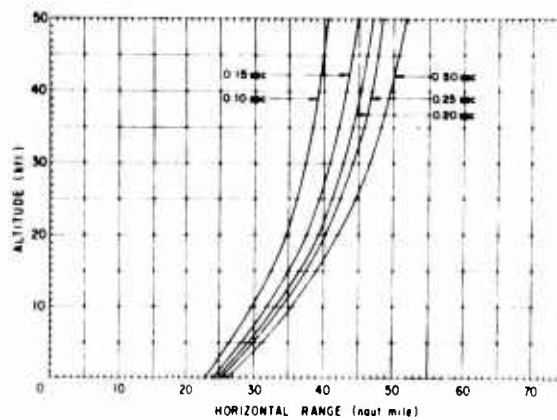
20C—Blink time, 0.1 sec. or more; 0.01-KT detonation at 1,000 ft.; night; 100-km. visibility.



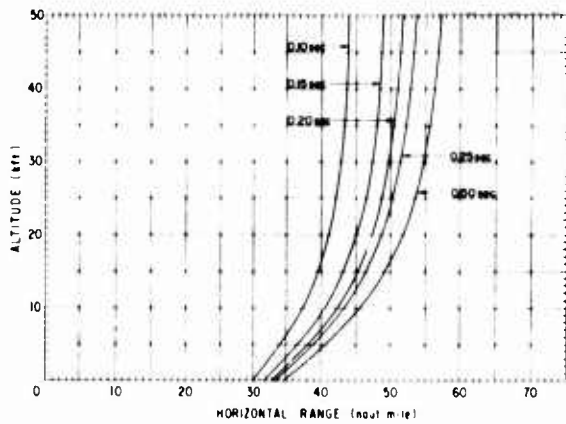
23C—Blink times, 0.1 and 0.15 sec. or more; 0.1-KT detonation at 10,000 ft.; night; 100-km. visibility.



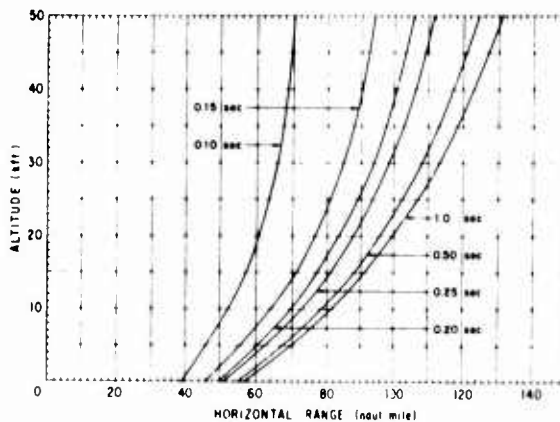
21C—Blink time, 0.1 sec. or more; 0.01-KT detonation at 10,000 ft.; night; 100-km. visibility.



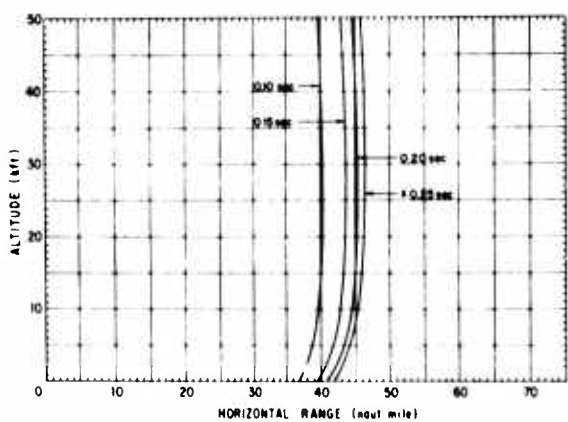
24C—Various blink times; 1-KT detonation at 1,000 ft.; night; 100-km. visibility.



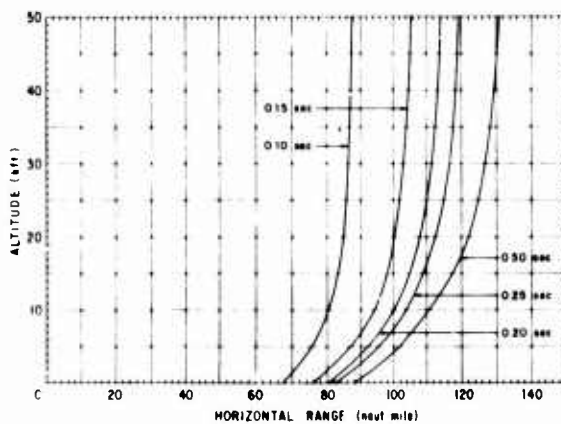
25C—Various blink times; 1-KT detonation at 10,000 ft.; night; 100-km. visibility.



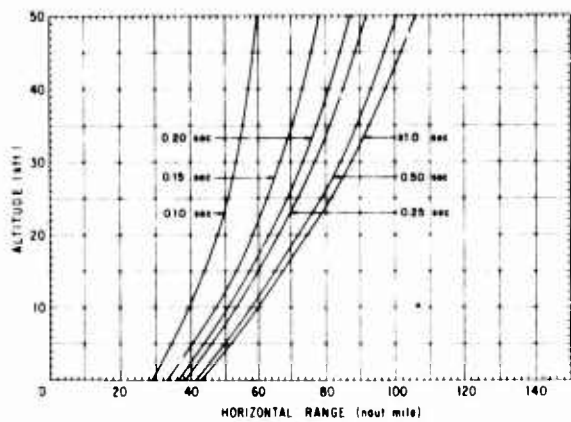
28C—Various blink times; 10-KT detonation at 10,000 ft.; night; 100-km. visibility.



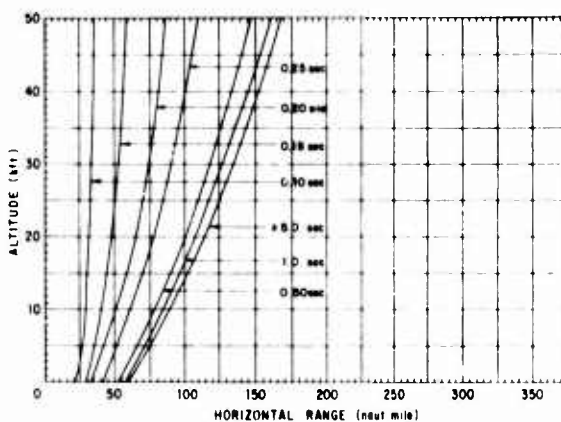
26C—Various blink times; 1-KT detonation at 50,000 ft.; night; 100-km. visibility.



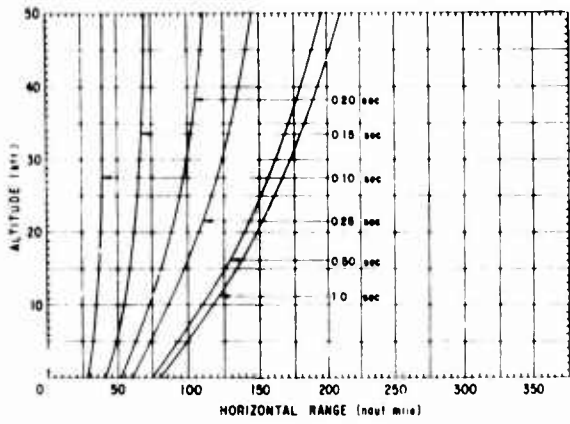
29C—Various blink times; 10-KT detonation at 50,000 ft.; night; 100-km. visibility.



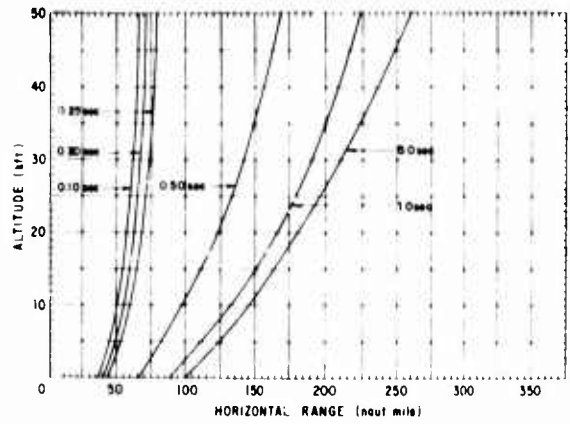
27C—Various blink times; 10-KT detonation at 1,000 ft.; night; 100-km. visibility.



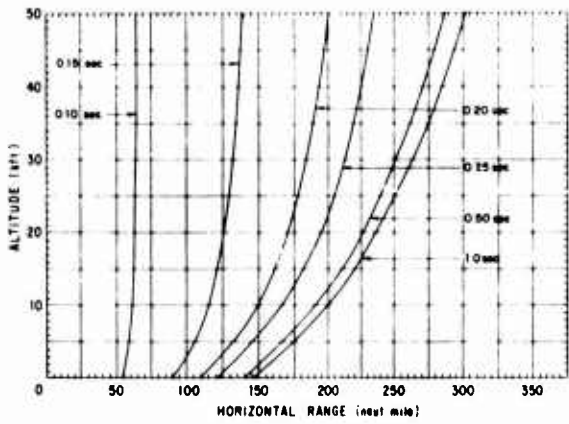
30C—Various blink times; 100-KT detonation at 1,000 ft.; night; 100-km. visibility.



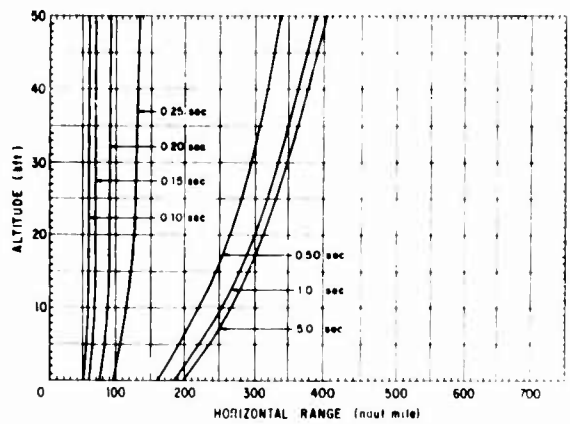
31C—Various blink times; 100-KT detonation at 10,000 ft.; night; 100-km. visibility.



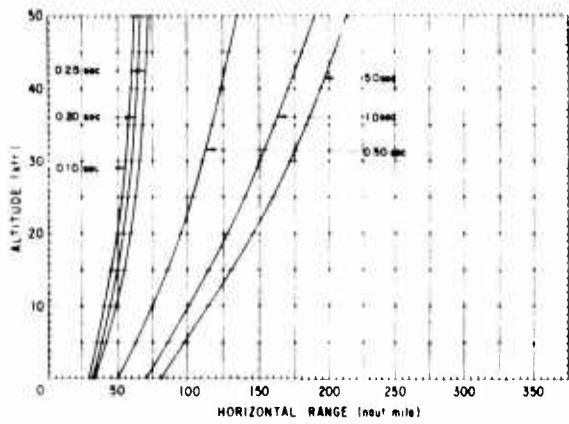
34C—Various blink times; 1,000-KT detonation at 10,000 ft.; night; 100-km. visibility.



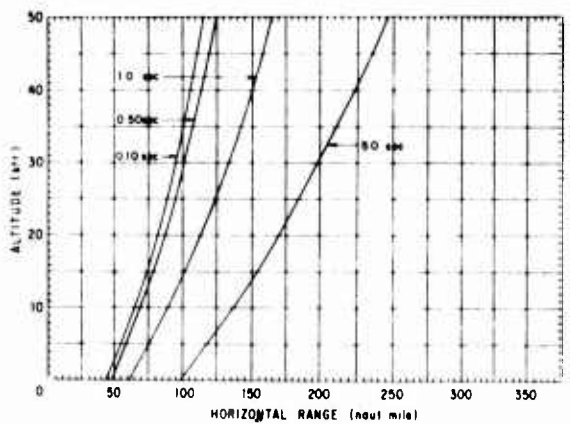
32C—Various blink times; 100-KT detonation at 50,000 ft.; night; 100-km. visibility.



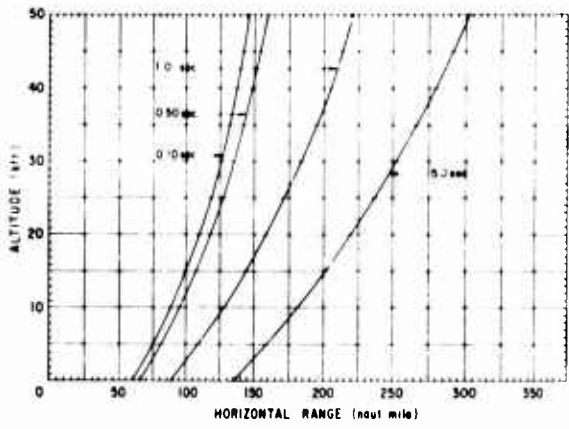
35C—Various blink times; 1,000-KT detonation at 50,000 ft.; night; 100-km. visibility.



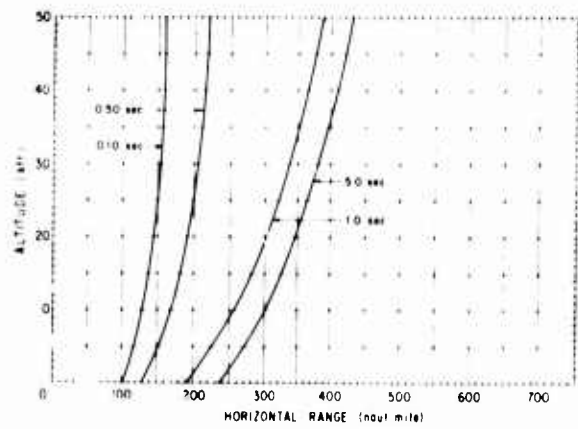
33C—Various blink times; 1,000-KT detonation at 1,000 ft.; night; 100-km. visibility.



36C—Various blink times; 10,000-KT detonation at 1,000 ft.; night; 100-km. visibility.



37C—Various blink times; 10,000-KT detonation at 10,000 ft.; night; 100-km. visibility.



38C—Various blink times; 10,000-KT detonation at 50,000 ft.; night; 100-km. visibility.

Unclassified
Security Classification

DOCUMENT CONTROL DATA - R & D

Security classification of title, body of abstract and indexing annotation must be entered when the overall report is classified.

1. ORIGINATING ACTIVITY (Corporate author) Technology Incorporated Life Sciences Division San Antonio, Texas		2a. REPORT SECURITY CLASSIFICATION Unclassified	
		2b. GROUP	
3. REPORT TITLE THE CALCULATION OF RETINAL BURN AND FLASHBLINDNESS SAFE SEPARATION DISTANCES			
4. DESCRIPTIVE NOTES (Type of report and inclusive dates) Summary report Nov. 1966 - Feb. 1968			
5. AUTHOR(S) (First name, middle initial, last name) R. G. Allen D. E. Jungbauer T. J. White J. H. Tips D. J. Isgitt E. O. Richey			
6. REPORT DATE September 1968	7a. TOTAL NO. OF PAGES 47	7b. NO. OF REFS 19	
8a. CONTRACT OR GRANT NO.		9a. ORIGINATOR'S REPORT NUMBER(S) SAM-TR-68-106	
b. PROJECT NO. 6301		9b. OTHER REPORT NO(S) (Any other numbers that may be assigned this report)	
c. Task No. 630103 DASA project 5710			
d. Subtasks RMD 2003 and RMD 2134			
10. DISTRIBUTION STATEMENT This document has been approved for public release and sale; its distribution is unlimited.			
11. SUPPLEMENTARY NOTES		12. SPONSORING MILITARY ACTIVITY USAF School of Aerospace Medicine Aerospace Medical Division (AFSC) Brooks Air Force Base, Texas	
13. ABSTRACT <p>This report describes a method for calculating safe separation distances from a nuclear fireball from the standpoint of permanent injury (chorioretinal burns) and temporary effects (flashtblindness). Weapon characteristics, atmospheric transmission, and the interaction of radiant energy with the eye are discussed. Predicted safe separation distances from a nuclear flash for humans are presented as functions of observer altitude, height of burst, weapon yield, and day or night conditions.</p>			

DD FORM 1 NOV 65 1473

Unclassified
Security Classification

14 KEY WORDS	LINK A		LINK B		LINK C	
	ROLE	WT	ROLE	WT	ROLE	WT
Ophthalmology Retinal burns Flashblindness Nuclear flash effects Safe separation distances from nuclear flash Eye effects from nuclear flash						